

Marina Lebedeva, Yury Yatsuk,  
Albert Khomyakov, Aleksey Lebedev,  
Andrey Afanasiev, Anastasiya Vasilieva,  
Konstantin Ushakov, Arkady Vetoshkin

## **WP3: INLAND WATERWAY VESSEL CONCEPTS PART1**

Project Future Potential of Inland Waterways (INFUTURE)

Financed by EU, Russian Federation and Republic of Finland



CBC 2014-2020  
SOUTH-EAST FINLAND - RUSSIA



**Admiral Makarov SUMIS**

**St. Petersburg 2019**

# CONTENTS

	<b><i>INTRODUCTION</i></b>	3
<b>1</b>	<b>Study of needs for new types of ships basing on the needs for new cargo flow servicing</b>	4
	1.1. Fleet analysis for the period 2018–2030	4
	1.2. Determination of technical and operational characteristics of ships optimized for the carriage of goods along lines connecting the inland waterways of Russia and Finland	11
	1.2.1. Determination of a round trip time when transporting goods along the considered lines	11
	1.2.2. Determination of the construction cost of new generation ships	16
	1.2.3. Determination of ship displacement and main dimensions	19
	<b><i>Conclusions Part 1</i></b>	29
<b>2</b>	<b>Development of analytical tools for the analysis of navigation on inland waterways</b>	30
	2.1. Methodology for assessment of the ship safety during maneuvering in narrow conditions	30
	2.1.1. Mathematical model of a ship	30
	2.1.2. Forces and moments acting on the ship	32
	2.1.3. Validation of the mathematical model for adequacy	36
	2.2. Procedure for analyzing the possibility of the ship passage along the Saimaa Canal	41
	<b><i>Conclusions Part 2</i></b>	50
<b>3</b>	<b>The study of main motion parameters of ships in open water</b>	51
	3.1. Propulsion qualities of ships	51
	3.2. Propulsion/steering unit	54
	<b><i>Conclusions Part 3</i></b>	61
<b>4</b>	<b>Comparison of old types of Saimaa max ships and some concept projects</b>	62
	<b><i>Conclusions Part 4</i></b>	65
	<b><i>REFERENCES</i></b>	66

## INTRODUCTION

The solution of the problem of designing and building cost-effective new generation vessels requires a preliminary study of a number of issues including the following:

- compliance assessment of the total carrying capacity of ships operating on the considered line, and the volume of cargo currently being transported, as well as the planned traffic volume;
- calculation of the designed ship construction and operation cost;
- assessment of navigation safety in the navigation area, including issues of maneuvering in confined areas, collision avoidance actions during encounters and overtaking, issues of autonomous mooring in wind conditions, etc.; safety inspection of navigation in ice conditions;
- evaluation of propulsion and steering capabilities of the actual ships, determination of parameters requiring improvement, and planning of improvement activities;
- analysis of the actual ships and determination of the advanced ship dimensions.

The analysis was performed at the first work stage, and its results are provided below in this report.

This report contains first year interim report on the WP3 of the **“Future potential of inland waterways, INFUTURE”** project, fulfilled by Admiral Makarov SUMIS research team in the period November 2018 – October 2019.

# **1 STUDY OF NEEDS FOR NEW TYPES OF VESSELS BASING ON THE NEEDS FOR NEW CARGO FLOW SERVICING**

## **1.1. Fleet analysis for the period 2018–2030**

The great majority of ships currently involved in the carriage of goods between the ports of the North-Western region of Russia and ports located within the Saimaa water system were built before 1995. The lack of newbuilding ships is explained, on the one hand, by the fact that the carrying capacity of the fleet involved is currently sufficient to support the existing cargo flows, and, on the other hand, the fact that relatively small ships suitable for operation within the Saimaa water system will inevitably lose in economic efficiency compared to large ships operating on other lines.

The steady aging of ships that comply with the restrictions imposed by the overall dimensions of the Saimaa water system locks in the medium term will lead to the fact that the construction of new cargo ships suitable for transportation along the Saimaa Canal will be on the agenda. In this part of the work, an attempt is made to predict the terms of disposal of the existing fleet of Russian cargo ships capable of carrying out cross-border transportation between Russia and the ports of the Saimaa water system.

Currently the following existing ships of the following types could be involved in transportation on the considered lines: ST-700, Fin-1000, Bakhtemir (STK) and ST-1300.

**ST-700** type is represented by ships of 276 and 2760 projects. These are German-built dry cargo ships (dwt 700 tons): four holds with hatch covers, aft-engined and aft superstructure. Project 2760 is characterized by modernized superstructure and afterpart. The ships were built from 1949 (Project 276) and from 1955 (Project 2760) till 1968; total built of 121 units. Years of construction completion from 1949 to 1968.

Type **Fin-1000** is represented by projects 540, 800, TY-3-100A — dry cargo ships with deadweight of 1,000 tons. Years of construction completion from 1958 to 1965.

Project Fin-1000/540 is a dry cargo ship with a capacity of 540 hp (397 kW), single-deck single-screw ship with closed-type holds, aft-engined and aft superstructure. Purpose: transportation of general cargo, grain, timber and bulk cargo. Place of build: Hollming Works Oy (Finland, Rauma) Ship Class: M

Project Fin-1000/800 is a dry cargo ship with a capacity of 800 hp, twin-screw ship, aft-engined and aft superstructure, with three cargo holds. Purpose: transportation of timber and general cargo. Place of build: Oy Laivateollisuus Ab (Finland, Turku). Ship Class: M

Project TY-3-100A is a dry cargo ship with a capacity of 800 hp (588 kW), single deck screw ship with closed holds, aft-engined and aft superstructure. Purpose: transportation of general and bulk cargo. Place of build: Oy Laivateollisuus Ab (Finland, Turku). Ship Class: O

Motor ships of the **Bakhtemir (STK)** type, projects 326 and 326.1 are medium-sized dry cargo ships and mixed-river-sea container ships with deadweight of 1,000 tons, closed-type holds, two decks, superstructure in the central part, and aft-engined. Years of construction completion from 1978 to 1989. Ship Class: M-IIP.

Dry cargo ships, Project 326 with two holds were also built. Project 326.1 is a modernized version adapted for the transportation of containers in the hold and on hatch covers and characterized by modified structural details of the superstructure and afterpart. In the 90s of the XX century, most ships underwent modernization to increase the deadweight, during which galleries on the lower deck were plated and high bulwarks on the foredeck were equipped.

Motor ships **ST-1300** (Project 191, Project 19620, Project R-168/K-90) are medium-sized dry-cargo ships of the river-sea class, having hold with hatch covers, two decks, bow superstructure and aft engine room. Years of construction completion — from 1983 to 1994. In the 1990s and 2000s, many ships were

modernized to increase the deadweight, galleries on the lower deck were plated and high bulwarks on the foredeck were equipped. Carrying capacity — 1,300 tons.

Estimation of the service life (age) of ships was carried out according to published sources [7]. Ships with a known history were accepted for consideration. It is assumed that the distribution of service lives is subject to normal law, with the main characteristics: the average value and the root mean square (RMS) acceleration.

To confirm the possibility of using the normal law of random variable distribution, data were used on the same type ships, Project 932 [7], with carrying capacity of 1,000 tons. All ships of this project are completely disposed, which makes it possible to obtain an untruncated law of time distribution before the ship disposal.

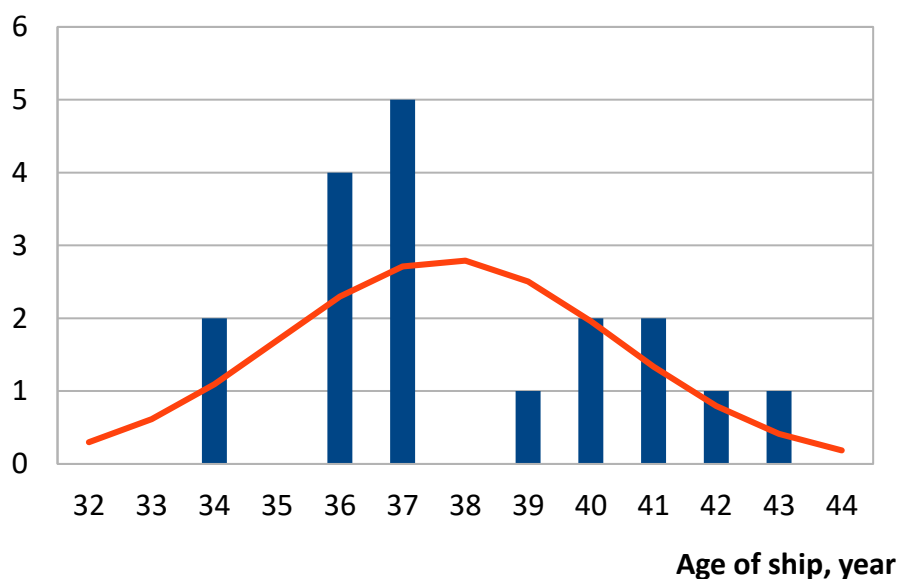


Fig. 1.1. Distribution of service life (age) before disposal, Project 932  
 At the x-axis — service life of ship/age of ships,  
 at the y-axis — number of disposed ships

In total, data of 18 ships with a reliable history and disposed at the end of the operation period were considered. The distribution of the service life (age) before disposal is shown in Figure 1.1. The distribution is approximated by a

normal law with the parameters: mathematical expectation  $MO = 37.7$  and standard deviation  $RMS = 2.7$ . To confirm the likelihood of the hypothesis about the consistency of theoretical and statistical distributions, the Pearson's chi-squared criterion was used [1]. As a result of the calculations, the value of the Pearson's criterion  $\chi^2$  is equal to 12.3 at which the probability value  $p$  is 0.33. By analyzing the result ( $p$  greater than 0.1), it can be said that the hypothesis of using the normal distribution law does not contradict the experimental data [1], therefore, the normal distribution law can be applied to all the ships considered herein.

The ships of the following types were considered: 1) ST-700, 2) Fin-1000, 3) Bakhtemir (STK), 4) ST-1300.

To determine the service life (age) of the ships, data were used [7], which were approximated by the normal distribution law based on the foregoing. Figures 1.2 through 1.5 show parts of the integral functions of the normal distribution law from the beginning of the service life (age) of ships to their disposal. Since some ships are in operation, the law is truncated. The truncation time of the approximated law shows the actual operating time of the set of ships before disposal, at the time of data processing. The law parameters and the truncation moment (actual operating time) are presented in Table 1.1.

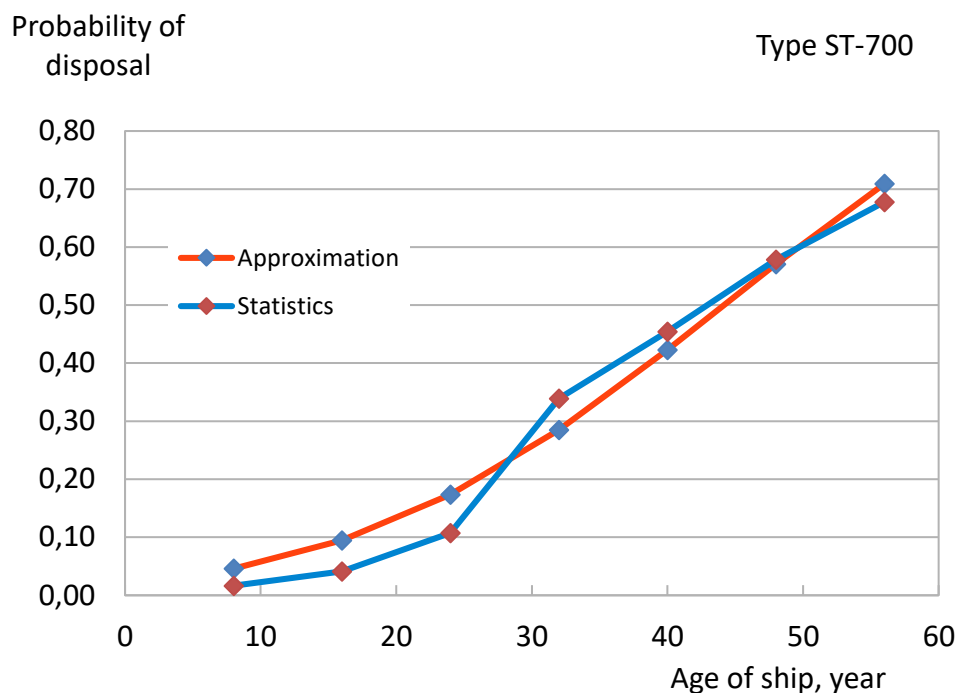


Fig. 1.2. Integral function of service life (age) distribution before disposal, Project ST-700

Further extrapolation of the disposal probability is carried out on the basis of the revealed parameters of the normal distribution law for ships of each type. The calculation of disposal of ships is determined by reducing the mathematical expectation by the value of the actual operating time. All calculation results are a matter of judgment.

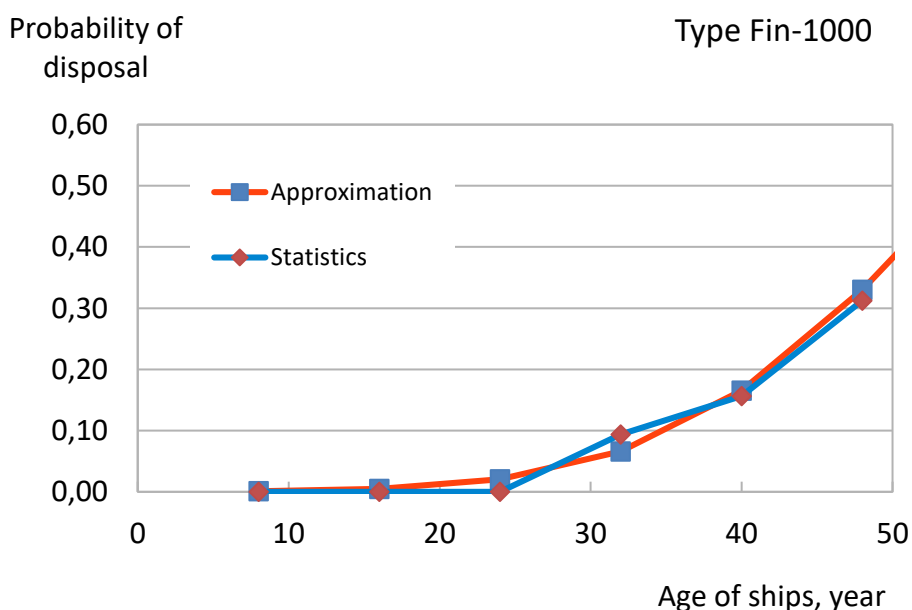


Fig. 1.3. Integral function of service life (age) distribution before disposal, Project Fin-1000



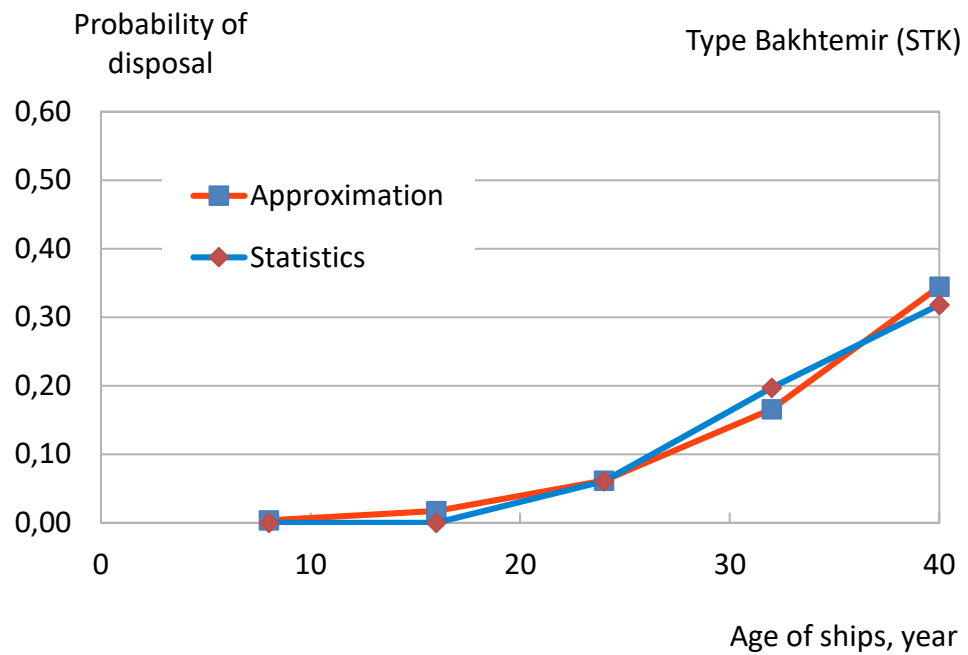


Fig. 1.4. Integral function of service life (age) distribution before disposal, Project Bakhtemir (STK)

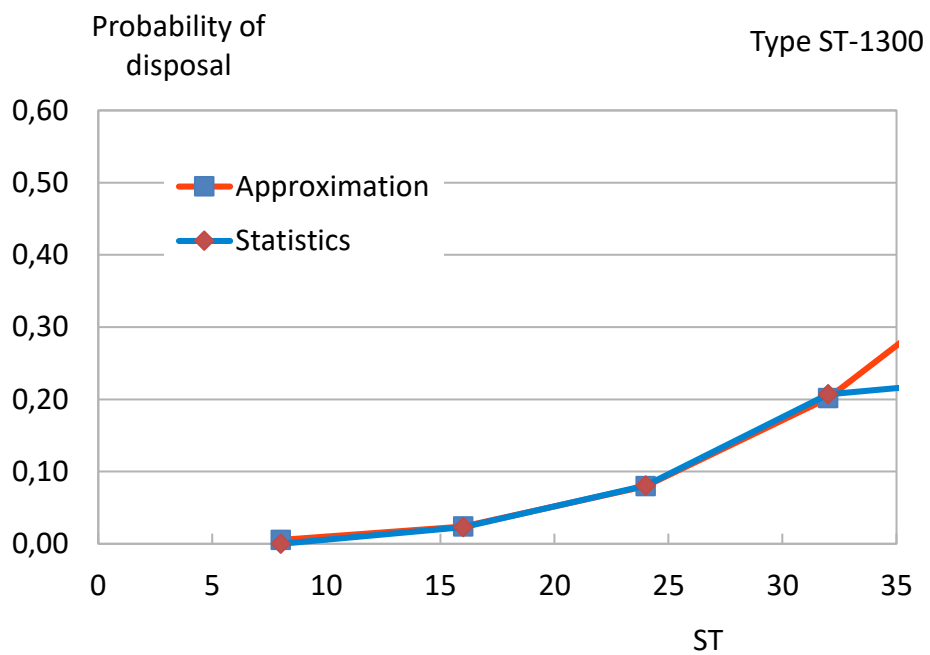


Fig. 1.5. Integral function of service life (age) distribution before disposal, Project ST-1300

Table 1.1 *The results of the study on the service life (age) determination at the end of 2018*

Type	Ships were built, un.	Ships in operation, un.	Average service life, years	RMS, years	Actual operating time, years
ST-700	121	36	44,2	21,5	57
Fin-1000	32	24	54,6	15	48

Bakhtemir (STK)	66	45	45,6	14	40
ST-1300	87	67	43,7	14	34

Estimation of the number of ships remaining in operation for the period until 2050 is presented in Table 1.2 and Figure 1.6.

Table 1.2 *Number of ships by years*

Ship type	2018	2026	2034	2042	2050
ST-700	36	22	12	6	0
Fin-1000	24	17	10	4	2
Bakhtemir (STK)	45	29	16	6	2
ST-1300	67	48	29	14	5
Sum	171	116	65	30	9

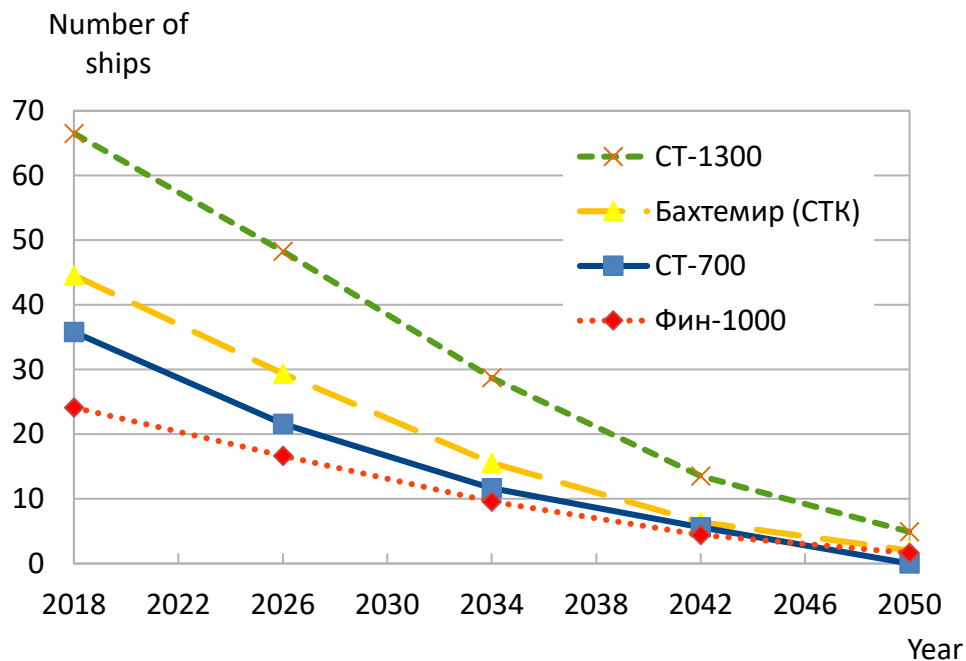


Fig. 1.6. Ships disposal by years

The results presented in Table 1.2 to be interpreted as follows.

- since the assessment is optimistic, it can be assumed that there will be no more ships than those indicated in Table 1.2.
- the assessment is biased due to the use in the calculation of time intervals equal to eight years, which also leads to a decrease in the number of serviceable ships.

Thus by 2030 the number of ships of the Russian river fleet suitable for operation on lines connecting the ports of the northwestern region of Russia with the ports of the Saimaa water system will be reduced almost by half. Similarly the total deadweight of ships will change.

The situation in the considered segment of ships as a whole is typical for the modern Russian fleet of inland and mixed navigation [24]. It can be noted that the measures taken by the Russian government aimed at stimulating shipbuilding bring certain results [27, 28]; however, currently the main attention of shipowners has been paid to modernization of larger vessels [25÷27] since they are more effective from a commercial point of view.

## **1.2. Determination of technical and operational characteristics of ships optimized for the carriage of goods along lines connecting the inland waterways of Russia and Finland**

### ***1.2.1. Determination of a round trip time when transporting goods along the considered lines***

Considering that most of the ships operating on the lines connecting Russia and Finland were built over thirty years ago, the designing and construction of new cargo ships optimized for operation on the considered lines will be on the agenda in the near future. To assess the technical and operational characteristics of new generation ships, it is necessary to obtain data on the organization of existing cargo ships operation.

The round trip duration depends not only on the ship speed and the distance between the ports of departure and arrival, but also on a number of other factors that can hardly be affected by shipowners and shipbuilders. Such factors include, for example, the unavoidable delays in transit associated with lockage, and the time of cargo handling operations, which is determined by the port equipment characteristics.

During the study, using the [marinetraffic.com](http://marinetraffic.com) service [8], data were collected on 104 voyages of 28 ships within the Saimaa water system along the

routes Vyborg-Lappeenranta and Lappeenranta-Imatra. The following were recorded: time (duration) of ship arrival, departure, passing the port without visit. The results of the study are presented below in Figures 1.7, 1.8, 1.9, and 1.10.

The analysis showed that the median trip time by the considered ships is equal to as follows:

from St. Petersburg to Vyborg — 13 hours 22 minutes;

from Vyborg to Lappeenranta — 8 hours 47 minutes;

from Lappeenranta to Imatra — 3 hours 19 minutes.

The total median trip time from St. Petersburg to Imatra is 25 hours 28 minutes.

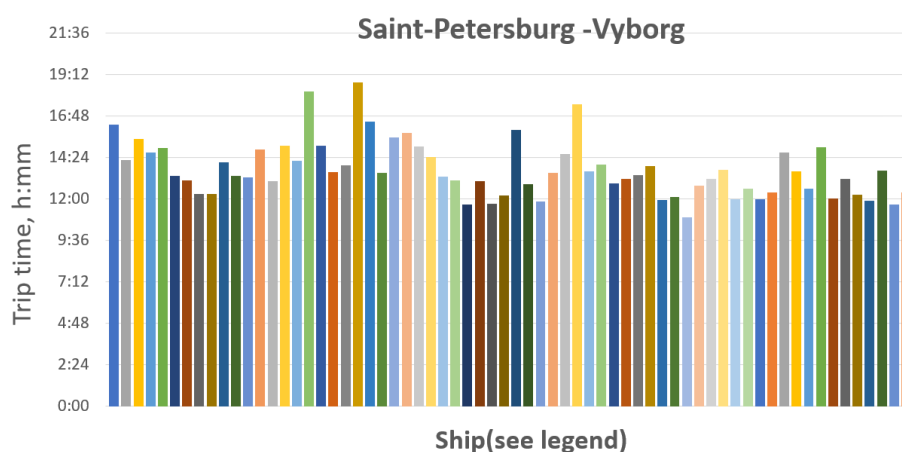


Fig. 1.7 Trip time of ships on the section St. Petersburg — Vyborg

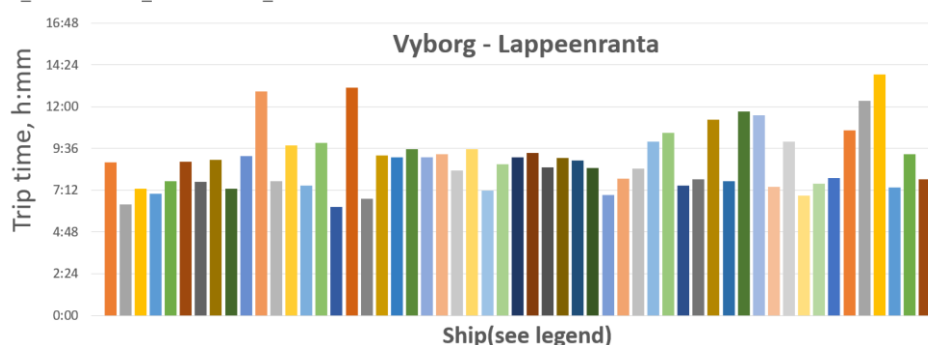
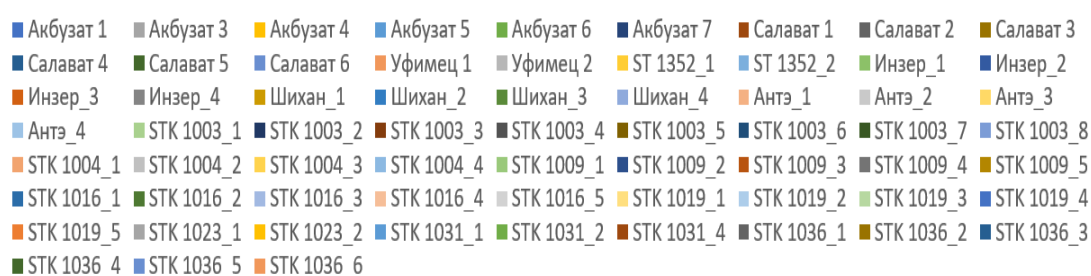


Fig. 1.8. Trip time of ships on the section Vyborg — Lappeenranta

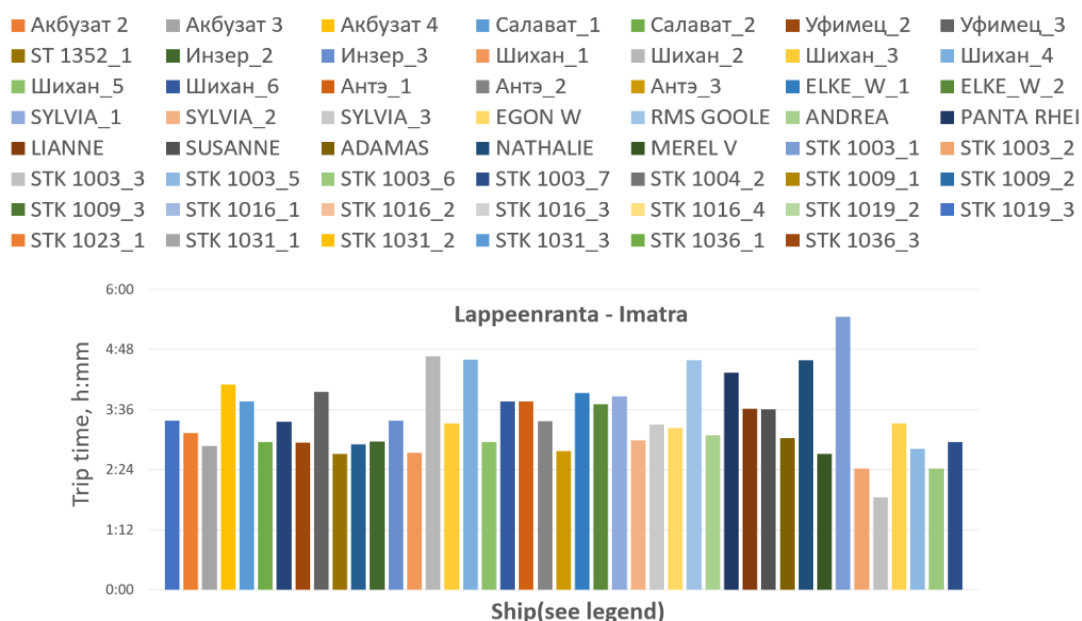


Fig. 1.9. Trip time of ships on the section Lappeenranta — Imatra

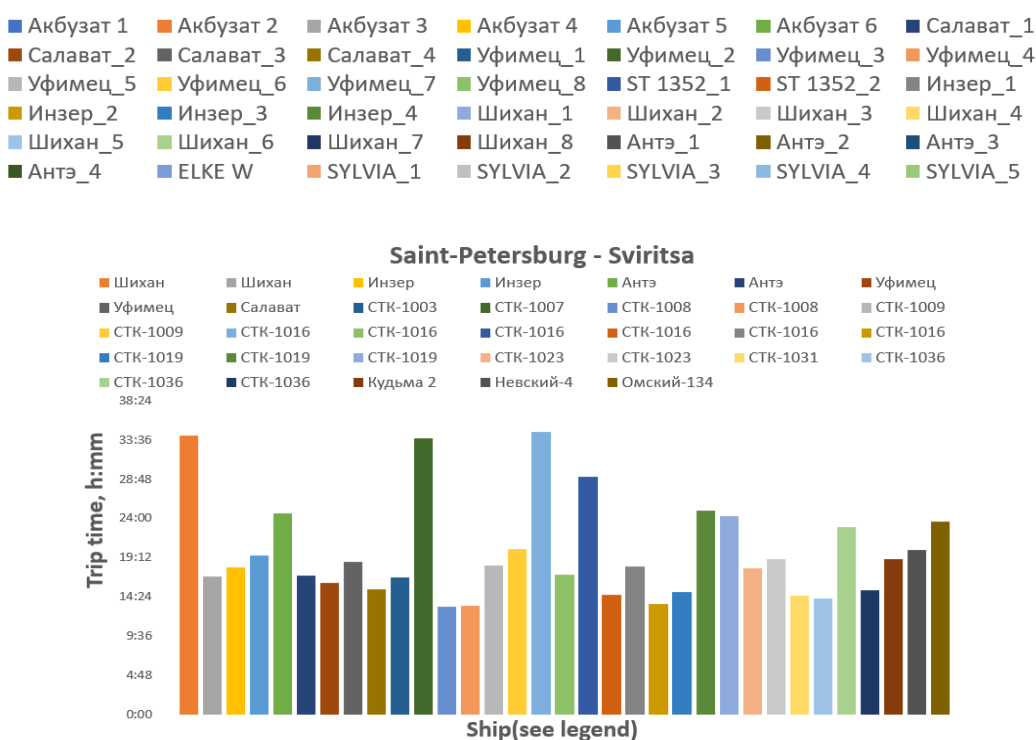


Fig. 1.10. Trip time of ships on the section St. Petersburg — Sviritsa

To analyze the movement of ships on the inland waterways of the Russian Federation, data were used that were posted on the Volgo-Balt Administration [2] website in the public domain. For the convenience of analysis, the ship passages of ports and settlements on the sections St. Petersburg — Sviritsa, Sviritsa — Vytegra, Vytegra — Annenskiy Most, Annenskiy Most — Cherepovets, and

Annenskiy Most — Mondoma were recorded. In total, data were obtained on 223 voyages of 75 ships, the overall dimensions of which correspond to the sizes of the modernized locks of the Saimaa Canal or slightly exceed them. Data on the time the ships pass along sections of the Volga-Baltic Waterway are presented in Figures 1.11 through 1.13.

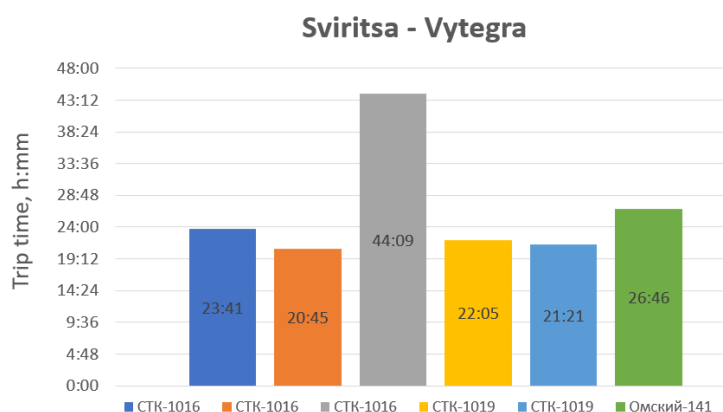


Fig. 1.11. Trip time of ships on the Sviritsa — Vytegra section

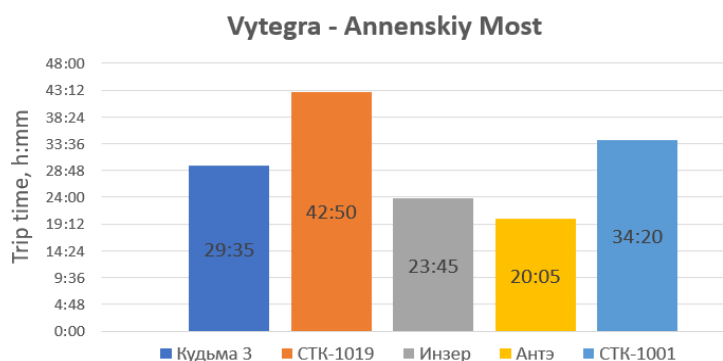


Fig. 1.12. Trip time of ships on the Vytegra — Annenskiy Most section

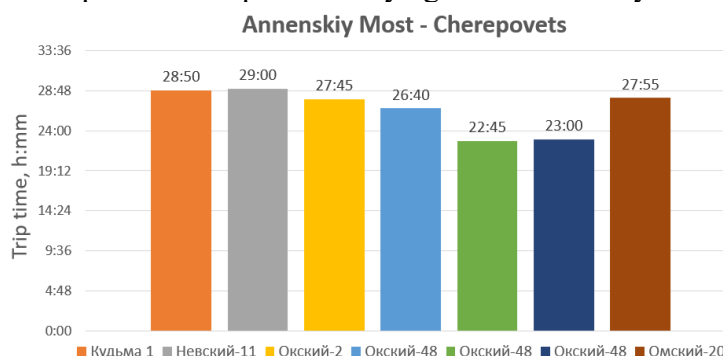


Fig. 1.13. Trip time of ships at Annenskiy Most — Cherepovets section

The analysis showed that the total median trip time of the considered ships, in particular, is:

- on the route St. Petersburg — Cherepovets — 98 hours 19 minutes;

- on the route St. Petersburg — Mondoma — 77 hours 51 minutes;

As the analysis showed, the actual time spent by the considered ships on moving along the Volga-Baltic waterway, in general, corresponds to the Ship routing standards presented on the Volgo-Balt Administration website [4]. The collected data on the length of the stay of the considered ships in the ports of Imatra and Lappeenranta are presented in Table 1.3.

Table 1.3 *Ship berthing time in the ports of Imatra and Lappeenranta*

<b>Imatra</b>		<b>Lappeenranta</b>	
UFIMETS (1)	21:07	STK 1003	7:48
UFIMETS (2)	8:56	STK 1003	15:42
UFIMETS (3)	19:33	STK 1003	4:28
AKBUZAT (1)	33:17	STK 1003	8:17
AKBUZAT (2)	9:31	STK 1016	12:18
AKBUZAT (3)	15:47	STK 1016	8:51
SHIKHAN (1)	10:42	STK 1016	11:05
SHIKHAN (2)	33:08	STK 1009	9:17
SHIKHAN (3)	11:47	STK 1009	22:51
SALAVAT (1)	21:00	STK 1019	8:51
SALAVAT (2)	13:23	STK 1019	16:24
ANTE (1)	10:05	SALAVAT	11:58
ANTE (2)	20:07	SALAVAT	13:32
SYLVIA (1)	25:00	STK 1004	11:43
SYLVIA (2)	20:13	STK 1023	8:32
SUSANNE (1)	17:53	STK 1031	19:52
CASE-13	9:30	STK 1036	8:37
ADAMAS	42:52	LIANNE	12:13
ST 1352	17:30	NATHALIE	13:40
INZER	28:46	<b>Median</b>	11:43
<b>Median</b>	18:43		

Table 1.4 *Ship berthing time in the ports of the North-West of Russia*

<b>Mondoma</b>		<b>Bely Ruchey</b>		<b>Vytegra</b>	
Shikhan	14:25	STK-1004	13:20	STK-1023	21:00
Shikhan	26:09	STK-1004	12:44	STK-1036	13:49
Inzer	19:33	STK-1031	10:30	<b>Median</b>	17:24
Ante	22:53	<b>Median</b>	12:44		
Ante	34:29				
Ufimets	17:03				
<b>Median</b>	21:13				

Data on the berthing time at the ports of the North-Western region of Russia are presented in Table 1.4. Unfortunately, the presented data do not allow to separately determine the time of cargo handling and technological operations, such as mooring, from the ship downtime.

### ***1.2.2. Determination of the construction cost of new generation ships***

Ships of new projects are built quite rarely, therefore, from the point of view of industry; they are products of piece and small batch production. Differences in the cost of equipment installed on the ship and technological features of the production of various shipbuilding enterprises lead to the fact that the cost of building ships with similar ship service characteristics, but built at different yards can vary significantly. For example, the cost of building a tanker of RST27 project at the Okskaya shipyard in 2012 amounted to 590.7 million rubles, and the cost of building a tanker for the same project at the Kherson Shipyard a year later was only 532.8 million rubles. It is also known that the cost of building the first ship of the series can be 20 ... 25% higher than the cost of subsequent ships of the series.

As a rule the cost of building a ship is finally determined upon agreement and a trade secret is considered. In the course of the work published data were collected and analyzed on the contract value of inland and mixed river-sea ships for various purposes built over the past fifteen years in Russia and neighboring states. The data obtained were considered as the contract price of the ship construction, excluding customs duties, as well as leasing payments and loan payments. In cases where the ship construction cost was indicated in rubles or dollars, it was converted into euros in accordance with the exchange rate of the Central Bank of the Russian Federation for the year of construction.

In Table 1.5 and in Figure 1.14 the collected data on the construction cost of dry cargo ships are presented. Data on the construction cost for tugboats depending on the power of the main engines and the construction cost for dry cargo barges are presented in Figures 1.15. and 1.16.



Table 1.5  
*Construction cost of dry cargo ships*

Project	Shipbuilder	Class	Speed, knots	Length, m	Breadth, m	Draft, m	Deadweight, t	No. of engines	1x engine power, kW	Year of construction	1x ship construction cost, mln €
DCV36	Qingdao Hyundai Shipbuilding	KM (*)Ice3 AUT1	12	89.96	14.5	6.4	5026	1	2640	2011	6.13
DCV47	Sosnovsky Ship-building yard (Russia, Sosnovka)	KM (*) Ice 2 [1] R1 AUT3	9	42.6	8.82	2	203	2	265	2012	3.20
RSD44	Oskaya Shipyard	O-ΠP 2,0 A (Ice 20)	10.5	139.99	16.8	3.527	5439	2	1200	2011	10.41
RSD49	Lotos Ship-building yard	KM Ice2 R2	11.5	139.95	16.5	4.7	7154	2	1200	2012	10.01
005RSD03	Onezhsky Ship-building yard	KM(*) Ice2[1] R2	10.5	108.3	16.5	4.79	5467	2	1020	2009	7.46
RSD17	Krasnoye Sormovo	KM(*) ЛУ2 I A1	11.5	121.7	16.5	5.06	6271	1	2450	2006	11.47
RSD18	China, Huaxia Shipping-Business CO., LTD(Wuhan), RU-WH01	KM (*) Ice1 R2 II AUT3	10.5	123.18	16.7	4.2	5189	2	956	2011	8.42
00101 Русич (Rusich)	Saigon Shipbuilding Industry Company	KM(*) ЛУ2[1] I A1	11	128.2	16.74	4.34	5190	2	1140	2009	9.20
00101 Русич (Rusich)	Krasnoye Sormovo	R1	11	128.2	16.74	4.2	5190	2	1140	2004	7.46
17605	Verkhnekamsk Shipbuilding Complex	KM(*) Ice2 AUT1-C	11.3	127.3	16.6	5	6826	2	1150	2012	9.52

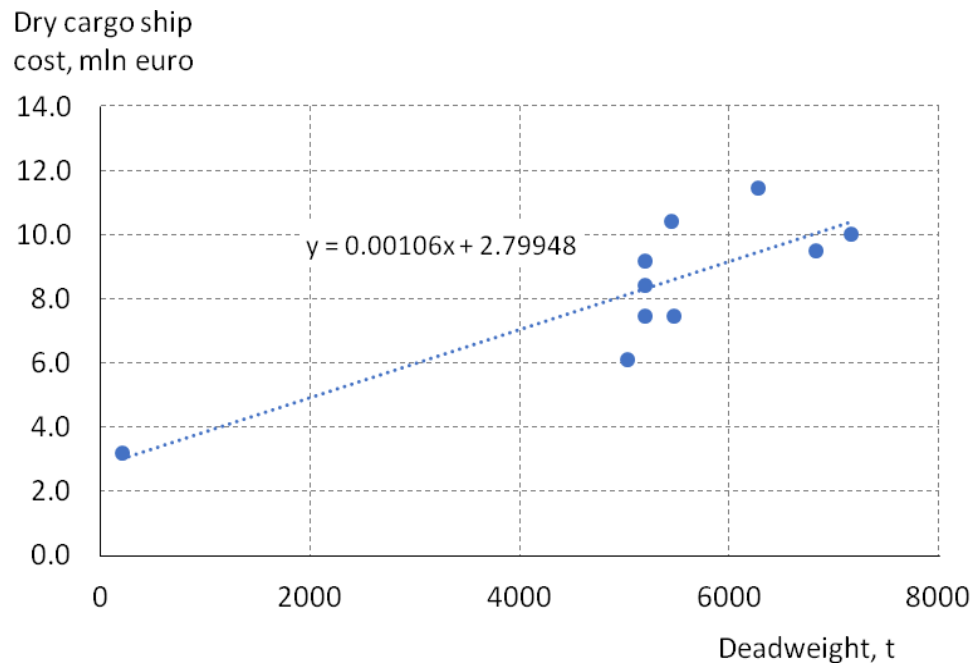


Fig. 1.14. The construction cost of dry cargo ships vs the deadweight

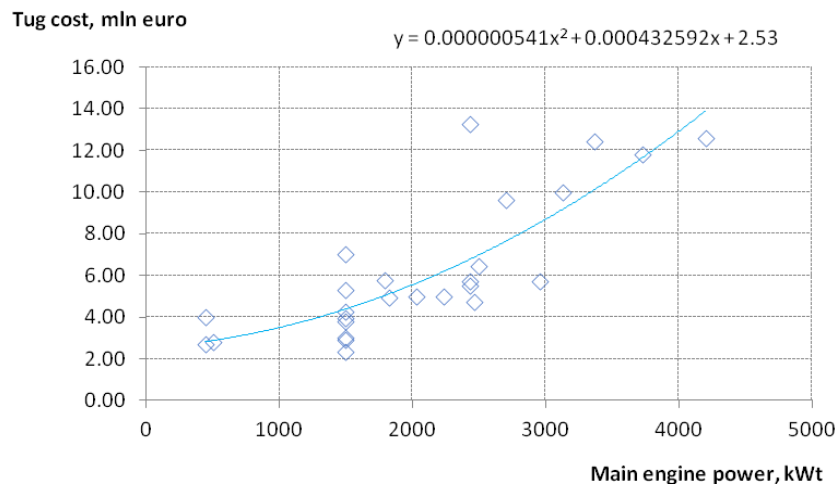


Fig. 1.15. The construction cost of tugs vs the power of the main engines

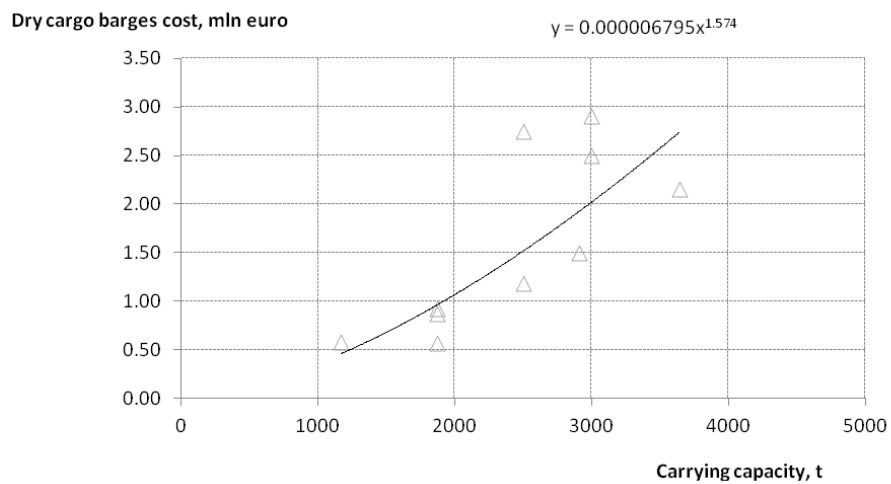


Fig. 1.16. The construction cost of dry cargo barges vs carrying capacity

### ***1.2.3. Determination of ship displacement and main dimensions***

The purpose of this phase of work was to determine the main characteristics of the new generation ships designed to operate on the line Saimaa Water System — Inland Waterways of Russia.

Access to the Saimaa water system is through a system of locks (the Saimaa Canal), and as a result the maximum dimensions of ships allowed into the system are limited in length to 82.5 meters, in width to 12.6 meters and in draft — to 4.35 meters. After the proposed modernization of the locks, the restrictions in the ship length will be 93.2 meters and in draft of 4.45 meters.

The waterways of the European Russia are connected into a single deep-sea system, which ensures guaranteed path depths up to four meters. Taking into account the required underkeel clearance, the desing draft of ships designed to operate on the considered lines shall not exceed 3.70 m.

In accordance with the Rules of the Russian River Register [6], ships designed to operate on the St. Petersburg – Vyborg line from April to November shall have a Class not lower than M-IIP (design wave height 3.0 m), and in case of year-round operation – not lower than M-CII (design wave height of 3.5 m). If the Russian Maritime Register of Shipping is selected as a classification society, the ship shall have a Class not lower than R3-RSN [5] for allowed operation in the considered water area. Considering that navigation in the inland waterways of the North-Western region of Russia in wintertime (from mid-November to the end of April) is not possible, the ships designed for operation in the region (Classes Ice 30 and Ice 40 of the Russian River Register or Class Ice 1 of the Russian Maritime Register of Shipping) are not advisable to sail in shallow ice with thickness of more than 30÷40 centimeters.

In order to assess possible solutions regarding the placement of premises for various purposes during the design of new generation ships, data were collected on the layout of modern dry cargo ships having dimensions close to those acceptable for the reconstructed Saimaa Canal. In the course of the collected data

analysis, three functional zones were allocated for each ship, schematically presented in Figure 1.17:

- fore-part limited to the rear by the forward bulkhead of the cargo hold;
- aft part limited in front by the aft bulkhead of the cargo hold;
- cargo area.

The analysis allowed to determine the estimated length of the aft part (Fig. 1.17), including the afterpeak and engine room, as well as the length of the fore part (Fig. 1.17).

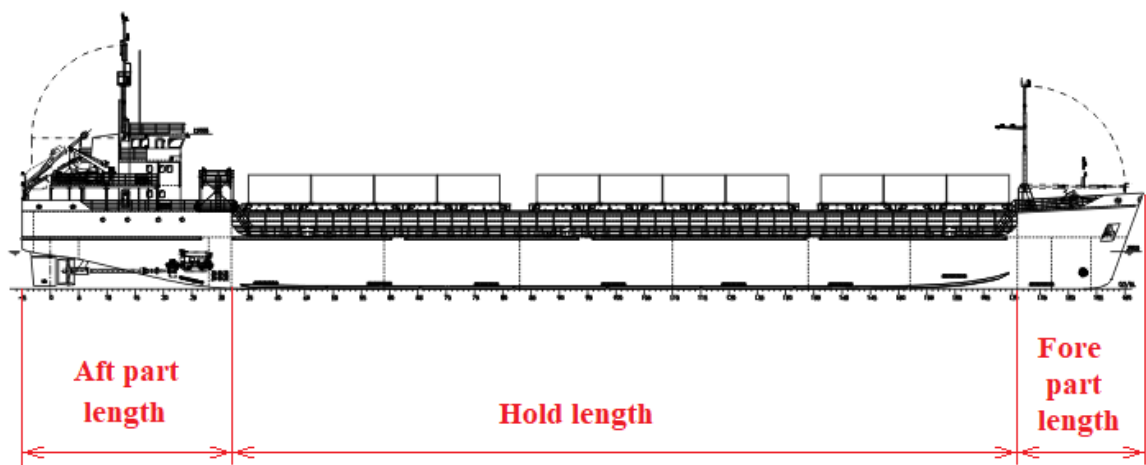


Fig. 1.17. The scheme of division of ship into functional zones

The collected data on the specific power of the ships of the considered class are presented in Figure 1.18 as the dependence of the Admiralty coefficient  $C_A = \Delta^{2/3} \cdot V_S^3 / P_S$  on the Block coefficient, where  $\Delta$  — ship displacement, tons;  $V_S$  — vessel speed, knots;  $P_S$  — main engine power, kW.

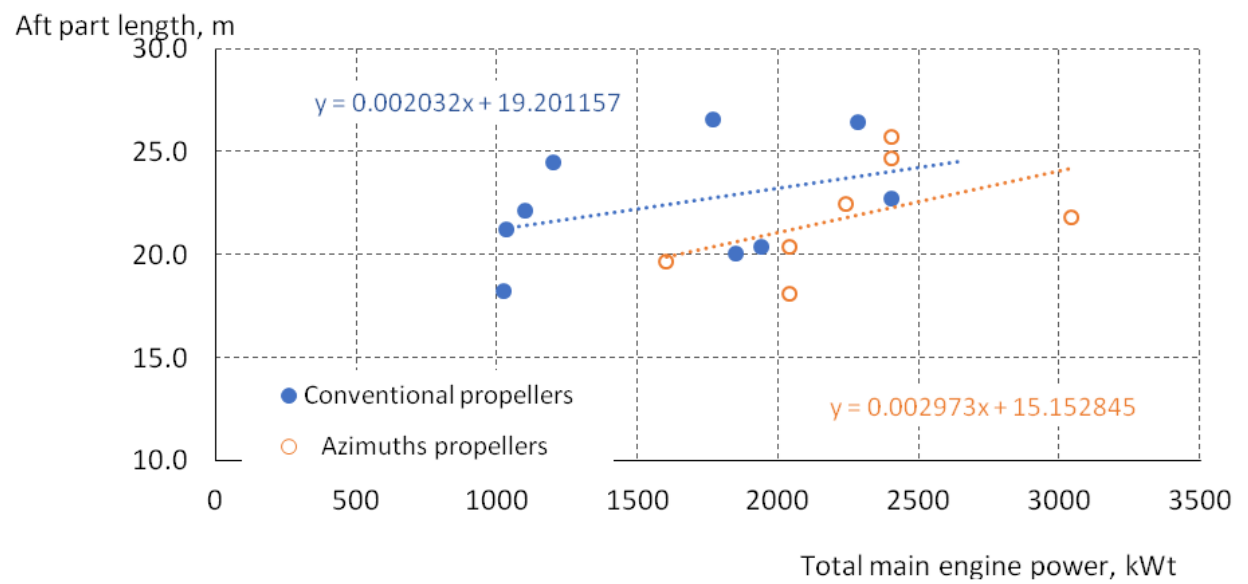


Fig. 1.18. Aft part length vs main engine power

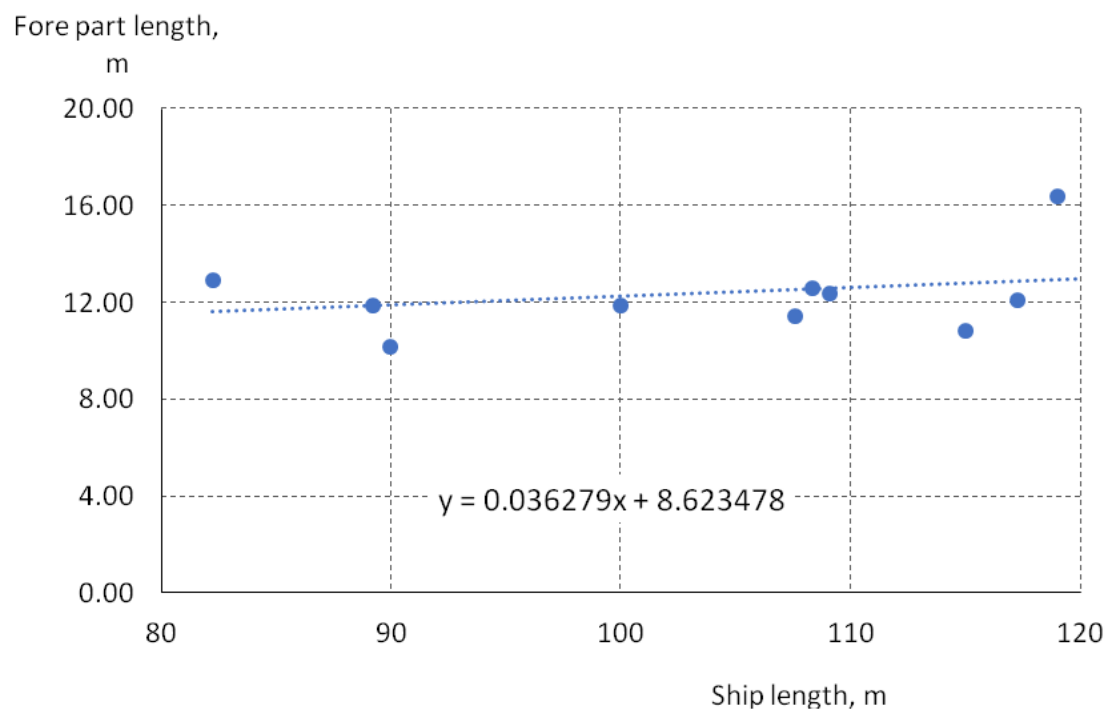


Fig. 1.19. Fore part length vs ship length overall

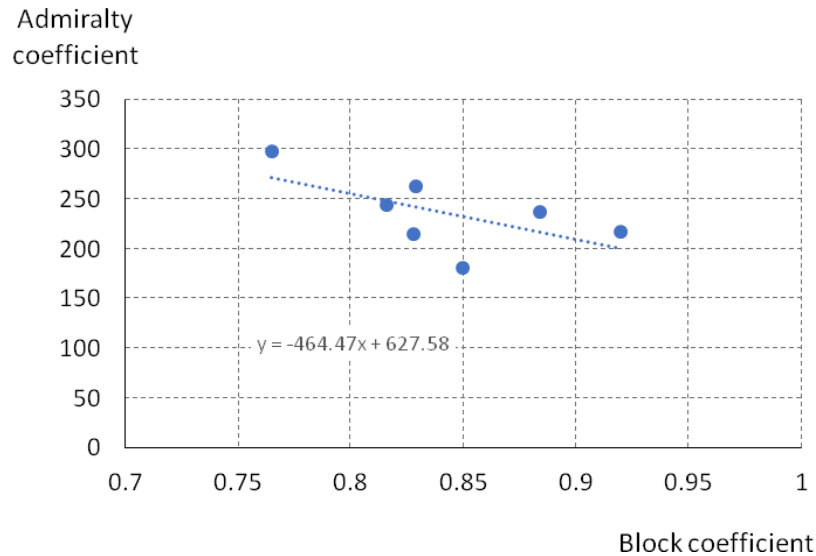


Fig. 1.20. Admiralty coefficient vs Block coefficient

A detailed analysis of design data on the hull weight of modern dry cargo ships and the weight of ship equipment was made by A. Egorov [3]. The author has proposed dependencies for the article-by-article calculation of the load of the designed ship as a first approximation at the initial design stage; as well as a structural analysis of the metal consumption of the hull structures was conducted.

In order to assess the ship maintenance cost, all operating expenses were divided into two categories:

- variable costs, including the cost of fuel and lubricating oil, and depending on the main engine power, the power of a constantly used diesel generator (100 kW was calculated), as well as the ratio of the movement time and downtime. Thus, variable costs directly depend on the considered line length and the time of the ship stay in ports;
- fixed costs, including salaries and crew nutrition, management, costs of inter-cruise and inter-navigation repairs, procurement of supplies, ship insurance and depreciation, as well as port charges.

During the calculations, it was assumed that the fuel and lubricating oil consumption is 0.196 kg/(kW·h), and the amount of fuel onboard at a time is sufficient to complete a round trip with a 10% margin.

The crew expenses is assumed to be 0.158 mln euro per navigation based on the crew of 10 people and includes both the actual salaries and overtime wages, vacation pay and the cost of meals. In the Russian Federation there is a provision in accordance with which mandatory payments to medical and social insurance funds for crew members of ships registered in the Russian International Ship Register are made by the state.

The costs of inter-cruise and inter-navigation repairs, the purchase of supplies, insurance and depreciation charges are estimated at a total of 6.05% of the ship cost per navigation. The value of port charges is estimated at 500 euro per voyage. The costs of corporate management are taken equal to 3% of the amount of expenses for crew remuneration, technical operation and insurance.

The collected data on the organization of transportation, ship weight and construction cost, as well as the cost of ship maintenance in operation, allow to solve the problem of determining the characteristics of a ship optimized for operation on the considered line. As the objective function when choosing the optimal ship, the transportation cost per ton, euro/t on the considered line was adopted. In this respect ships having the maximum permissible length (93.2 m) and width (12.5 m) for the reconstructed Saimaa Canal were considered. Draft was limited to 3.7 m, characteristic of the inland waterways of Russia. The scheme of the designed cross section of the considered series of ships is presented in Figure 1.21.

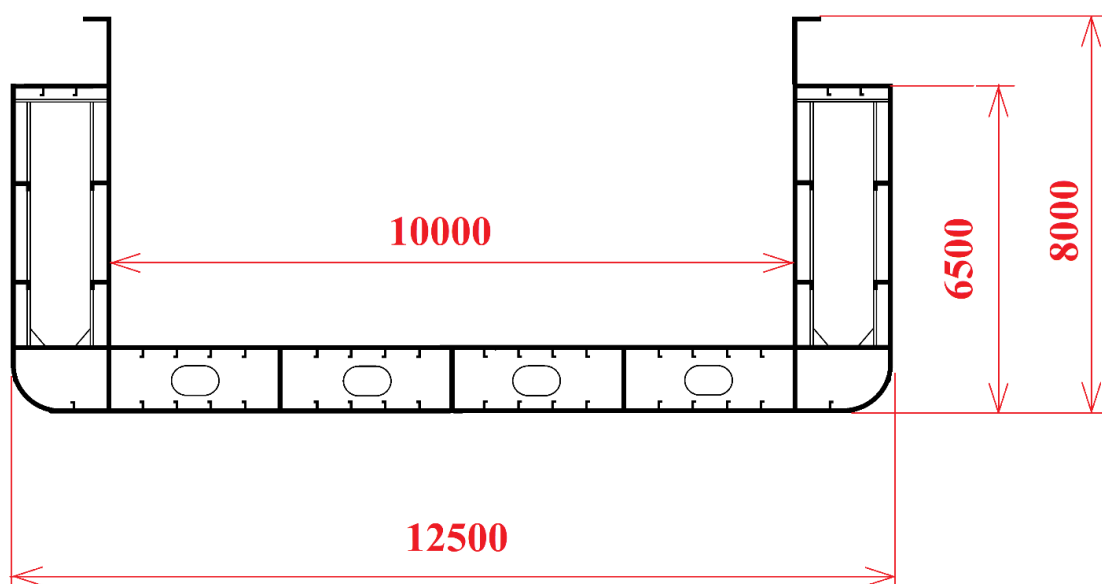


Fig. 1.21. The scheme of the designed cross section of the cargo ships of new generation

The block coefficient and the speed were used as variable parameters. Then displacement, required power of the main engines, hold dimensions, as well as weight of the hull, equipment, engines and stocks were determined.

Upon determination of the main technical characteristics, ship construction costs and operation costs including the salary, repair costs, consumables costs, insurance, depreciation, fuel and port charges.

The volume of cargo transported per navigation was determined in relation to the characteristic route, taking into account the ship speed and carrying capacity.

Figure 1.22 and Table 1.6 show the calculation results for the case of transporting timber cargo with a density of 0.43 t/m<sup>3</sup> on the Mondoma-Lappeenranta line at a design speed of 10 knots.

As follows from the results obtained, the optimal value of the block coefficient is 0.88. An increase in the block coefficient in excess of 0.91 or its decrease to values less than 0.82 leads to a noticeable increase in the transportation costs. Figure 1.22 also shows the results of comparing the transportation costs of one ton of timber cargo by ships that do not have an ice class and ships with Ice 2 class of the Russian Maritime Register of Shipping. It should be noted that this comparison is somewhat conditional since in both cases the navigation period was limited in accordance with the practice of navigation on the inland waterways of



the North-Western region of Russia and amounted to 200 days a year. As follows from the results obtained, the transportation cost when transition to ships with the ice class Ice 2 increases by about 1.5%.

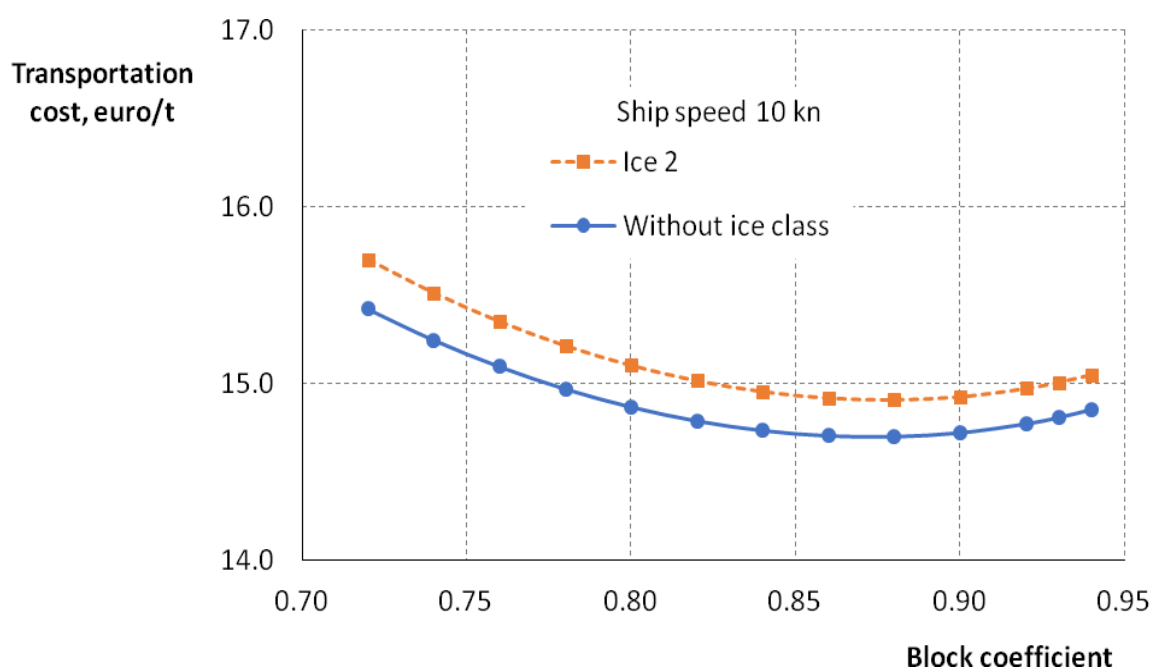


Fig. 1.22. The transportation cost of one ton of cargo along the Mondoma — Lappeenranta line, depending on the block coefficient and the ice class

Figure 1.22 compares the transportation cost of one ton of timber cargo along the Mondoma-Lappeenranta line by the ship with the traditional aft superstructure and the ship with a restricted air draft and bow superstructure. A ship with a restricted air draft is heavier, but when moving without deck cargo it has the ability to pass the Neva bridges without loss of time. As follows from the results obtained, a ship with a restricted air draft is more effective from a commercial point of view, but this gain is small and in practice the situation may be different. Further research is needed to decide which option should be preferred.

The conclusion that it is advisable to increase the block coefficient of inland and mixed navigation ships intended for the general cargo delivery corresponds to modern approaches to the design of ships of this class [16, 22, 23].

Table 1.6

*Determination of the transportation cost of one ton of timber cargo along the  
Mondoma-Lappeenranta line at a design speed of 10 knots*

Block coefficient	0.72	0.76	0.8	0.84	0.88	0.92	0.94
Engine power, kW	745.5	825.3	916.1	1020.6	1142.3	1286.1	1368.2
Afterpart length (conventional propellers), m	20.72	20.88	21.06	21.28	21.52	21.81	21.98
Forepart length, m	12.6	12.6	12.6	12.6	12.6	12.6	12.6
Hold length, m	59.90	59.74	59.56	59.35	59.10	58.81	58.64
Hold volume, m <sup>3</sup>	4792	4779	4765	4748	4728	4705	4691
Efficient hull height, m	7.73	7.73	7.73	7.72	7.72	7.71	7.71
Displacement, t	3103.6	3276.0	3448.4	3620.8	3793.2	3965.7	4051.9
Steel hull weight, t	463.8	489.4	514.9	540.3	565.7	591.0	603.5
Superstructure weight, t	90.4	90.4	90.4	90.4	90.4	90.4	90.4
Additional ice zone construction, t	0.0	0.0	0.0	0.0	0.0	0.0	0.0
Foundation weight, t	28.6	28.6	28.6	28.6	28.6	28.6	28.6
Tackle weight, t	13.4	13.4	13.4	13.4	13.4	13.4	13.4
Coloring & isolation weight, t	58.0	58.0	58.0	58.0	57.9	57.9	57.9
Equipment weight, t	26.4	26.4	26.4	26.4	26.4	26.4	26.4
Gears & systems weight, t	184.3	184.3	184.2	184.2	184.1	184.0	183.9
Engine room equipment weight, t	82.0	90.8	100.8	112.3	125.7	141.5	150.5
Fuel weight, t	18.5	20.2	22.1	24.4	27.0	30.1	31.9
Hull weight, t	947.0	981.3	1016.7	1053.6	1092.2	1133.1	1154.7
Cargo weight, t	2138	2274	2410	2543	2674	2802	2865
Cargo turnover per navigation, t	44899	47764	50600	53400	56155	58851	60172
Deadweight, t	2157	2295	2432	2567	2701	2833	2897

Table 1.6 continued

Block coefficient	0.72	0.76	0.8	0.84	0.88	0.92	0.94
Ship cost, mln. Euro	5.09	5.23	5.38	5.52	5.66	5.80	5.87
Cargo volume, cu.m	4960.27	5276.81	5590.12	5899.44	6203.74	6501.62	6647.55
Cargo height, m	8.28	8.83	9.39	9.94	10.50	11.06	11.34
Salary per navigation, mln euro	0.158	0.158	0.158	0.158	0.158	0.158	0.158
Inter-trip repair cost per navigation (0.25% of ship cost), mln euro	0.013	0.013	0.013	0.014	0.014	0.015	0.015
Regular repair cost per navigation (0.6% of ship cost), mln euro	0.031	0.031	0.032	0.033	0.034	0.035	0.035
Consumables cost (0.1% of ship cost), mln euro	0.005	0.005	0.005	0.006	0.006	0.006	0.006
Insurance cost (0.1% of ship cost), mln euro	0.005	0.005	0.005	0.006	0.006	0.006	0.006
Management cost (3% of Salary+Consumables+Insurance), mln euro	0.005	0.005	0.005	0.005	0.005	0.005	0.005
Depreciation deductions per navigation (5% of ship cost), mln euro	0.254	0.262	0.269	0.276	0.283	0.290	0.294
Fuel cost per navigation (600 euro per t), mln euro	0.212	0.231	0.254	0.279	0.310	0.345	0.365
Port charges per navigation, mln euro	0.011	0.011	0.011	0.011	0.011	0.011	0.011
First cost per navigation, mln euro	0.693	0.721	0.752	0.787	0.825	0.869	0.894
Transportation cost per ton, euro/t	15.42	15.10	14.87	14.73	14.70	14.77	14.85

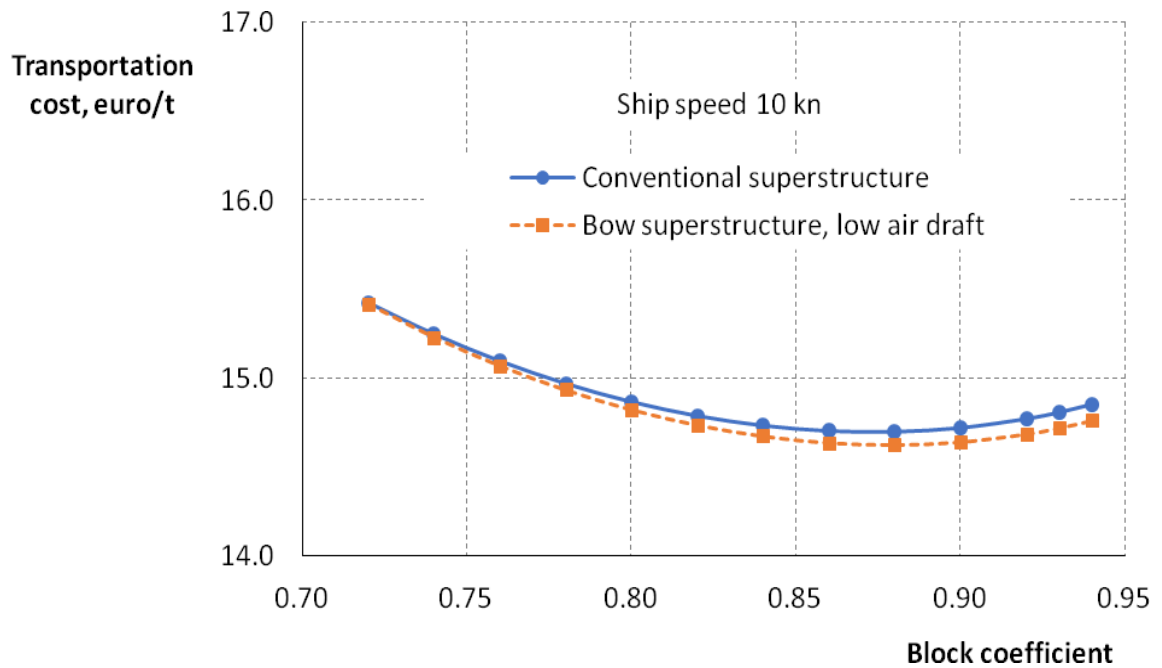


Fig. 1.23. The transportation cost of one ton of cargo along the Mondoma — Lappeenranta line, depending on the block coefficient and the air draft

Figure 1.24 shows the transportation cost of one 20-foot container with an average weight of 16 tons along the Lappeenranta-Moscow line. The design ship speed was assumed to be 12 knots, but it was believed that the average ship speed on the line increases by only 40% compared to the base speed of 10 knots and is 10.8 knots. This decrease in average speed was envisaged in order to take into account the downtime of ships when moving along inland waterways. As follows from figure 1.24, the optimal value of the block coefficient of the ship in this case is 0.76. An increase in the block coefficient compared with this value leads to a sharp increase in fuel costs, and a decrease leads to a decrease in the number of containers taken for transportation.

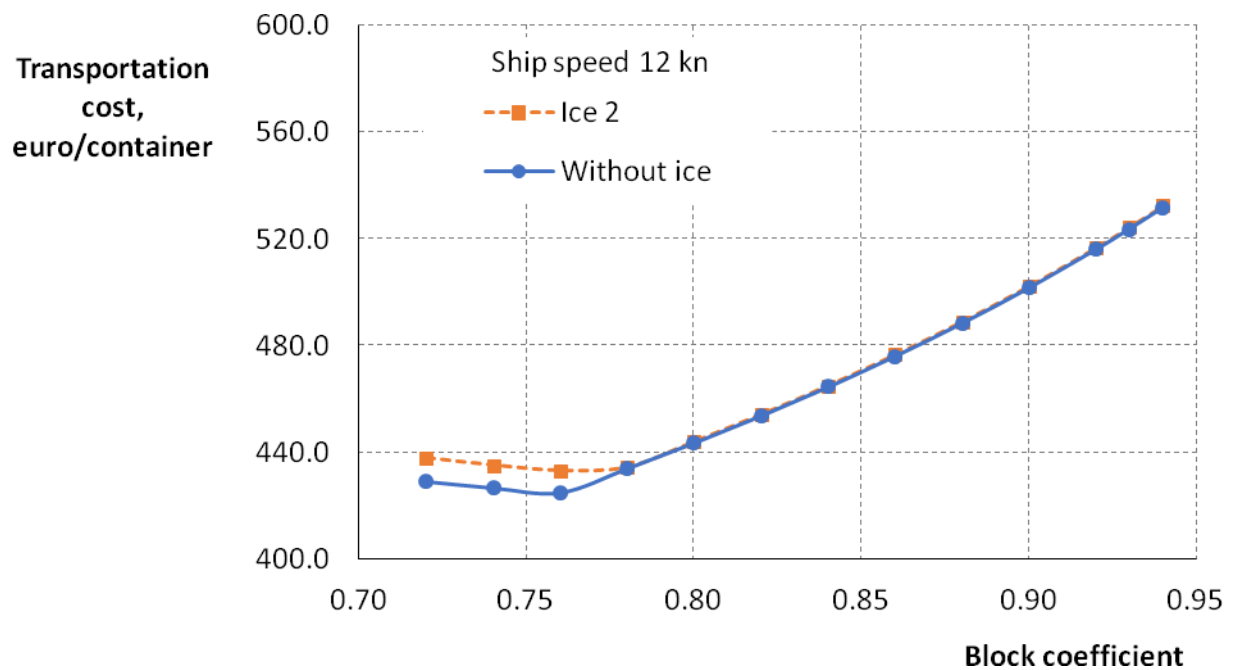


Fig. 1.24. The transportation cost of one container on the Lappeenranta — Moscow line, depending on the block coefficient

### CONCLUSIONS PART 1

1. By 2030 the number of ships of the Russian river fleet suitable for operation on lines connecting the ports of the northwestern region of Russia with the ports of the Saimaa water system will be reduced almost by half. Similarly the total deadweight of ships will change.
2. The optimal value of the ship block coefficient for timber transportation is 0.88. An increase in the block coefficient in excess of 0.91 or its decrease to values less than 0.82 leads to a noticeable increase in the transportation cost.
3. A vessel with a restricted air draft is heavier that leads to an increase in the transportation cost. But when moving without deck cargo it has the ability to pass the Neva bridges without loss of time. Thus a vessel with a restricted air draft is more effective from a commercial point of view, but this gain is small and in practice the situation may be different.
4. The optimal value of the block coefficient of the container ship is 0.76. An increase in the block coefficient compared with this value leads to a sharp increase in fuel costs, and a decrease leads to a decrease in the number of containers taken for transportation.

## 2. DEVELOPMENT OF ANALYTICAL TOOLS FOR THE ANALYSIS OF NAVIGATION ON INLAND WATERWAYS

During development a conceptual design of a new ship, along with characteristics of performance, economy, and environmental issues, we shall not forget about the navigation safety directly related to the above mentioned problems. This is especially important in conditions of a limited, practically closed water area, such as the Saimaa Canal. In case of a fuel spill due to a collision of ships, the consequences can be disastrous.

It is possible to increase in the transported cargo volume that requires a preliminary consideration of a number of scenarios of ship movement, including independent maneuvering, possibility of maneuvering using tugboats, limiting values of wind speed (minimum and maximum), etc.

Calculation of motion parameters of each ship shall be as accurate as possible.

### 2.1. Methodology for assessment of the ship safety during maneuvering in narrow conditions

#### 2.1.1. *Mathematical model of the ship*

The mathematical model of the ship is a system of 3 nonlinear differential equations of the first order of the following form [9], [10]:

$$\frac{dV_x}{dt} \cdot (m + \lambda_{11}) = \sum X_i, \quad (2.1)$$

$$\frac{dV_y}{dt} \cdot (m + \lambda_{22}) = \sum Y_i, \quad (2.2)$$

$$\frac{d\omega_z}{dt} \cdot (I_z + \lambda_{66}) = \sum M_i, \quad (2.3)$$

Where:  $V_x$ ,  $V_y$ ,  $\omega_z$  — longitudinal and lateral components of the speed in the coordinate system associated with the ship,  $m$  — ship mass,  $I_z$  — moment of

inertia of the ship relative to the vertical axis,  $\lambda_{11}$ ,  $\lambda_{22}$ ,  $\lambda_{66}$  — attached masses of the naked ship hull,  $\sum X_i$  — main vector of all forces acting in the centerline plane,  $\sum Y_i$  — main vector of all forces acting in the transverse sectional plane,  $\sum M_i$  — main vector of moments of all forces acting relative to the vertical axis. In the performance of the task two coordinate systems are used (Fig. 2): a fixed coordinate system ( $OX_0Y_0$ ) connected to the Earth, and a coordinate system ( $OX_1Y_1$ ) connected to the ship, the center of the latter coincides with the center of gravity of the ship.

The North direction is considered the positive direction of the  $X_0$  axis; the East direction is considered the positive direction of the  $Y_0$  axis.

The positive direction of the  $X_1$  axis is the forward direction, the positive direction of the  $Y_1$  axis is the direction toward the starboard side. Signs of hydrodynamic forces are considered positive if they act in the direction of the axes. The drift angle is considered positive if it is counted clockwise from the speed vector to the ship centerline plane.

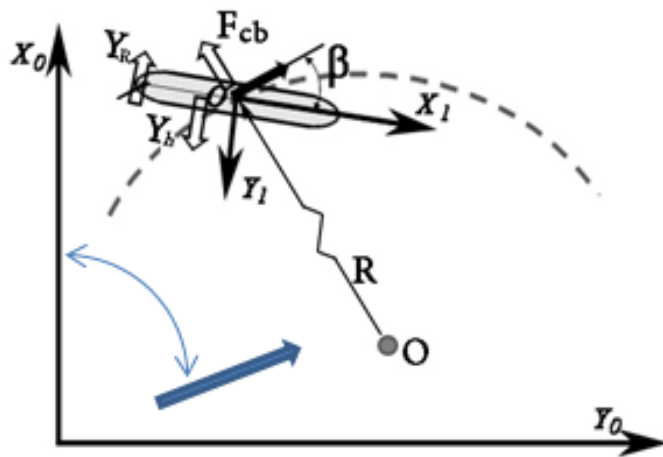


Fig. 2.1. Coordinate systems adopted in the calculation

The value and direction of the true wind speed acting on the ship is set in a fixed coordinate system. The components of the wind speed acting in the direction of the coordinate axes are considered positive. The course angle  $\psi$  is considered positive if it is counted clockwise from the  $X$  axis.

The values of aerodynamic forces and moments are determined depending on the relative wind angle, i.e. the angle between the true wind direction and the instantaneous position of the ship centerline plane [11].

Hydrodynamic and aerodynamic moments are considered positive if they act clockwise.

### ***2.1.2. Forces and moments acting on the ship***

The components of the forces and moments acting on the ship when moving in open water can be determined in the traditional way as follows

$$\sum X_i = X_{bh} + X_a + T_p, \quad (2.4)$$

$$\sum Y_i = Y_{bh} + Y_a + Y_R, \quad (2.5)$$

$$\sum M_i = M_{bh} + M_a + Y_R \cdot l_R, \quad (2.6)$$

Where  $X_{bh}$ ,  $Y_{bh}$ ,  $M_{bh}$  — longitudinal and lateral component of the hydrodynamic force and the hydrodynamic moment on the naked ship hull,  $X_a$ ,  $Y_a$ ,  $M_a$  — longitudinal and lateral component of the aerodynamic force and the aerodynamic moment on the above-water body,  $T_p$  — propeller thrust,  $Y_R$  — rudder lateral force,  $l_R$  — rudder arm.

The hydrodynamic force components and the hydrodynamic moment on the naked ship hull are calculated using databases

$$X_{bh} = C_{xbh}(\beta, \bar{\omega}) \cdot 0.5 \rho V_{sh}^2 \cdot LT, \quad (2.7)$$

$$Y_{bh} = C_{ybh}(\beta, \bar{\omega}) \cdot 0.5 \rho V_{sh}^2 \cdot LT, \quad (2.8)$$

$$M_{bh} = C_{mbh}(\beta, \bar{\omega}) \cdot 0.5 \rho V_{sh}^2 \cdot L^2 T, \quad (2.9)$$

Where  $C_{xbh}(\beta, \bar{\omega})$ ,  $C_{ybh}(\beta, \bar{\omega})$ ,  $C_{mbh}(\beta, \bar{\omega})$  — nondimensional components of the force and nondimensional moment on the naked ship hull (hydrodynamic characteristics of the hull),  $V_{sh}$  — ship speed,  $\rho$  — water density,  $L$  and  $T$  — length and draft of the ship.



Nondimensional hydrodynamic characteristics are determined depending on the drift angle  $\beta$  and the relative curvature of the trajectory  $\bar{\omega}$ .

Structural formulas for calculating the hydrodynamic characteristics of the hull and rudder are as follows:

- longitudinal component of hydrodynamic force

$$C_x(\beta, \omega) = C_x^0 + C_x^\beta \cdot \beta + C_x^{\beta\beta} \cdot \beta^2 + C_x^\omega \cdot \omega + C_x^{\omega\omega} \cdot \omega^2 + C_x^{\beta\omega} \cdot \beta\omega + C_x^{\beta\beta\omega} \cdot \beta^2\omega + C_x^{\beta\omega\omega} \cdot \beta\omega^2 + C_x^{\beta\beta\omega\omega} \cdot \beta^2\omega^2, \quad (2.10)$$

- lateral component of hydrodynamic force

$$C_y(\beta, \omega) = C_y^0 + C_y^\beta \cdot \beta + C_y^{\beta\beta} \cdot \beta^2 + C_y^\omega \cdot \omega + C_y^{\omega\omega} \cdot \omega^2 + C_y^{\beta\omega} \cdot \beta\omega + C_y^{\beta\beta\omega} \cdot \beta^2\omega + C_y^{\beta\omega\omega} \cdot \beta\omega^2 + C_y^{\beta\beta\omega\omega} \cdot \beta^2\omega^2, \quad (2.11)$$

- hydrodynamic moment

$$C_m(\beta, \omega) = C_m^0 + C_m^\beta \cdot \beta + C_m^{\beta\beta} \cdot \beta^2 + C_m^\omega \cdot \omega + C_m^{\omega\omega} \cdot \omega^2 + C_m^{\beta\omega} \cdot \beta\omega + C_m^{\beta\beta\omega} \cdot \beta^2\omega + C_m^{\beta\omega\omega} \cdot \beta\omega^2 + C_m^{\beta\beta\omega\omega} \cdot \beta^2\omega^2 \quad (2.12)$$

The formula for calculating the lateral force on the rudder is [9]

$$Y_R = C_{yR}^\delta \cdot \delta \cdot 0.5\rho V^2 L T, \quad (2.13)$$

Where  $C_{yR}^\delta$  — derivative of the lateral force with respect to the rudder angle,  $\delta$  — rudder angle. When calculating the lateral force on the rudder installed behind the propeller, the speed of the flow acting onto the rudder is calculated considering the speed caused by the propeller.

Propeller thrust is determined by formulas [12]

$$T_P = k_1(J_p) \cdot (1 - t_w) \cdot \rho \cdot n^2 \cdot D_p^4, \quad (2.14)$$

Where  $k_1(J_p)$  — propeller thrust coefficient,  $n$  — propeller speed,  $D_p$  — propeller diameter,  $t_w$  — thrust-deduction factor.

The value of the propeller thrust coefficient is calculated by the formula:

$$k_1(J_p) = 0.453 - 0.192 \cdot J_p - 0.11 \cdot J_p^2 \quad (2.15)$$

The values of the aerodynamic force components and the moment acting on the above-water body can be calculated according to the following relationships:

- longitudinal component of aerodynamic force

$$X_a = C_{Xa}(\gamma_k) \cdot 0.5 \rho_{\text{wind}} V_{\text{wind}}^2 \cdot A_x, \quad (2.16)$$

- lateral component of aerodynamic force

$$Y_a = C_{Ya}(\gamma_k) \cdot 0.5 \rho_{\text{wind}} V_{\text{wind}}^2 \cdot A_y, \quad (2.17)$$

- aerodynamic moment

$$M_a = C_{Ma}(\gamma_k) \cdot 0.5 \rho_{\text{wind}} V_{\text{wind}}^2 \cdot A_y \cdot L, \quad (2.18)$$

Where  $C_{Xa}(\gamma_k)$ ,  $C_{Ya}(\gamma_k)$ ,  $C_{Ma}(\gamma_k)$  — nondimensional values of the components of the force and moment on the above-water body (aerodynamic characteristics of the hull), depending on the ship motion parameters,  $V_{\text{wind}}$  — relative wind angle,  $\rho_{\text{wind}}$  — air density,  $A_x$  and  $A_y$  — sail area in the projection onto the midship frame plane and the centerline plane respectively.

The relative wind speed components are determined in a fixed coordinate system as the sum of the corresponding speed and wind components.

$$V_k^2 = (V_{Xsh} + V_{Xwind})^2 + (V_{Ysh} + V_{Ywind})^2, \quad (2.19)$$

Where  $V_{Xsh}$ ,  $V_{Xwind}$  — longitudinal components of the ship speed and the wind speed in a fixed coordinate system;  $V_{Ysh}$ ,  $V_{Ywind}$  — lateral components of the ship speed and the wind speed.

The values of the components of the speeds are determined by the following relationships

- ship speed

$$V_{Xsh} = V_0 \cdot \cos(\psi - \beta) - V_0 \cdot \sin(\psi - \beta) = V_0 \cdot [\cos(\psi - \beta) - \sin(\psi - \beta)] \quad (2.20)$$

$$V_{Ysh} = V_0 \cdot \sin(\psi - \beta) + V_0 \cdot \cos(\psi - \beta) = V_0 \cdot [\sin(\psi - \beta) + \cos(\psi - \beta)] \quad (2.21)$$

Where  $V_0$  — displacement speed of the ship center of gravity,  $\psi$  — current heading angle,  $\beta$  — drift angle.

- wind speed

$$V_{Xwind} = V_{\text{wind}} \cdot \cos \gamma_0 \quad (2.22)$$

$$V_{Ywind} = V_{wind} \cdot \sin \gamma_0 \quad (2.23)$$

Where  $V_{wind}$  — wind speed in the absolute coordinate system,  $\gamma_0$  — wind angle in a fixed coordinate system.

The apparent wind angle is determined as the ratio of lateral and longitudinal speed components. The formula for calculation is as follows

$$\gamma_k = \text{atg} \left( \frac{V_{Ysh} + V_{Ywind}}{V_{Xsh} + V_{Xwind}} \right) \quad (2.24)$$

If the wind speed is zero, then the apparent wind angle and speed will be equal to the drift angle and the ship speed.

To assess nondimensional aerodynamic characteristics, database [12] is used depending on the above-water outline profile of the ship.

Structural formulas for calculating the hydrodynamic characteristics of the hull and rudder are as follows:

- nondimensional longitudinal component of aerodynamic force

$$C_{xa} = -0.051 - [0.329 \cdot \cos(\gamma_k) + 0.045 \cdot \sin(\gamma_k)] - [0.032 \cdot \cos(2\gamma_k) + 0.267 \cdot \sin(2\gamma_k)] - [0.025 \cdot \cos(3\gamma_k) + 0.190 \cdot \sin(3\gamma_k)] - [0.023 \cdot \cos(4\gamma_k) + 0.136 \cdot \sin(4\gamma_k)] \quad (2.25)$$

- nondimensional lateral component of aerodynamic force

$$C_{ya} = 0.29 + [-0.017 \cdot \cos(\gamma_k) + 0.453 \cdot \sin(\gamma_k)] + [-0.183 \cdot \cos(2\gamma_k) - 0.013 \cdot \sin(2\gamma_k)] + [-0.0056 \cdot \cos(3\gamma_k) + 0.021 \cdot \sin(3\gamma_k)] + [-0.061 \cdot \cos(4\gamma_k) - 0.017 \cdot \sin(4\gamma_k)] \quad (2.26)$$

- nondimensional aerodynamic moment

$$C_{Ma} = -0.00025 + [0.039 \cdot \cos(\gamma_k) - 0.001 \cdot \sin(\gamma_k)] + [0.0016 \cdot \cos(2\gamma_k) + 0.046 \cdot \sin(2\gamma_k)] + [-0.024 \cdot \cos(3\gamma_k) + 0.00098 \cdot \sin(3\gamma_k)] + [0.000041 \cdot \cos(4\gamma_k) + 0.00047 \cdot \sin(4\gamma_k)] \quad (2.27)$$

To calculate the ship motion parameters in ice conditions, forces and moments caused by the ice influence shall be to the forces acting on the hull.

### ***2.1.3. Validation of the mathematical model for adequacy***

The conclusion about the correctness of the developed mathematical model is made on the basis of a comparison of the calculated motion parameters with the corresponding ship motion parameters obtained as a result of field tests.

For this purpose test calculations are performed. Test modes include

- the ship motion parameters at a steady turning;
- the ship motion parameters when entrance the turning;
- parameters of ship motion in unsteady maneuvering with the wind.

To assess the test mathematical model adequacy, a ship with the main dimensions corresponding to the future dimensions of the lock was chosen

- |                                      |         |
|--------------------------------------|---------|
| - maximum length                     | 93.0 m  |
| - length on waterline (LWL)          | 89.1 m  |
| - width                              | 12.6 m, |
| - construction waterline (CWL) draft | 4.45 m, |

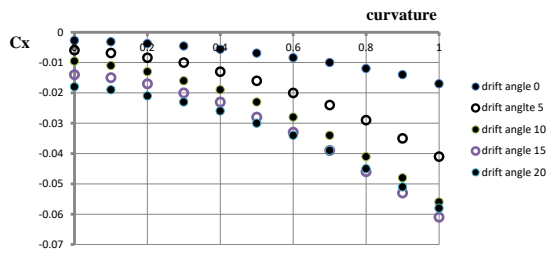
The ship was equipped with a balancing rudder mounted in the centerline plane behind the right rotating controllable-pitch propeller. The rudder area was 11 m<sup>2</sup>, the propeller diameter was 2.3 m.

The speed of fully-loaded estimated ship was 13.0 knots.

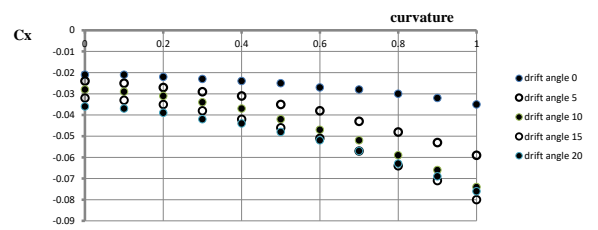
The calculations were performed for two trim options: fully-loaded with an even-keel trim (draft of 4.45 m) and in ballast trimmed by the stern (draft on the amidship of 2.45 m).

The hydrodynamic characteristics used for the calculations are shown in Figures 2.2 through 2.4.

On the graphs at the x-axis the values of the relative curvature of trajectory, and at the y-axis the corresponding values of hydrodynamic characteristics are plotted.

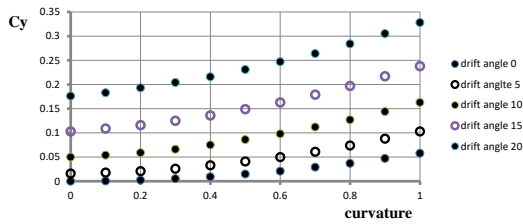


a) Fully-loaded

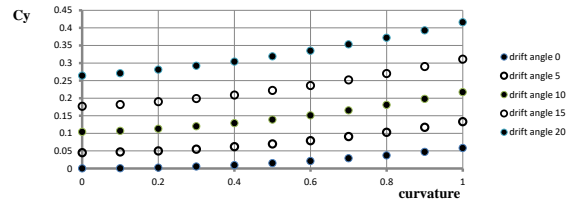


b) Ballasted

Fig. 2.2. Nondimensional longitudinal force

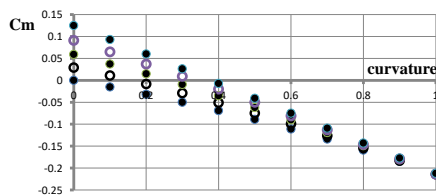


a) Fully-loaded

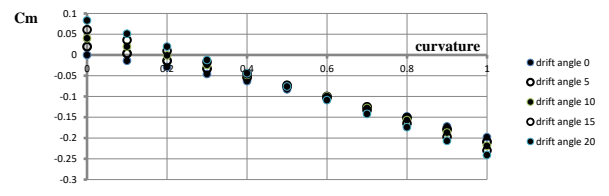


b) Ballasted

Fig. 2.3. Nondimensional lateral force



a) Fully-loaded



b) Ballasted

Fig. 2.4. Nondimensional hydrodynamic moment

**Calculation of steady turning parameters.** The results of calculation the relative curvature of trajectory  $\bar{\omega} = L/R$  at various rudder and drift angles are shown in Fig. 2.5 и 2.6

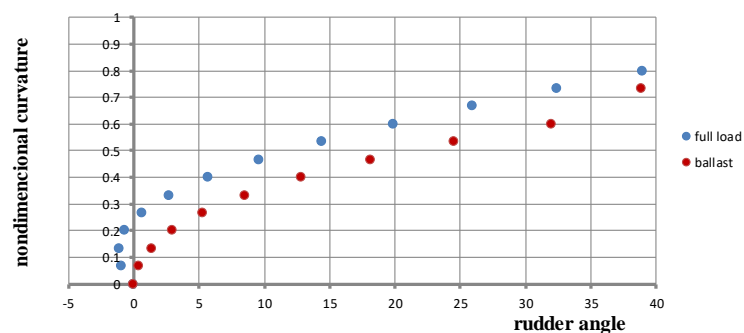


Fig.2.5. The relative curvature of trajectory at different rudder angles for two trim options.

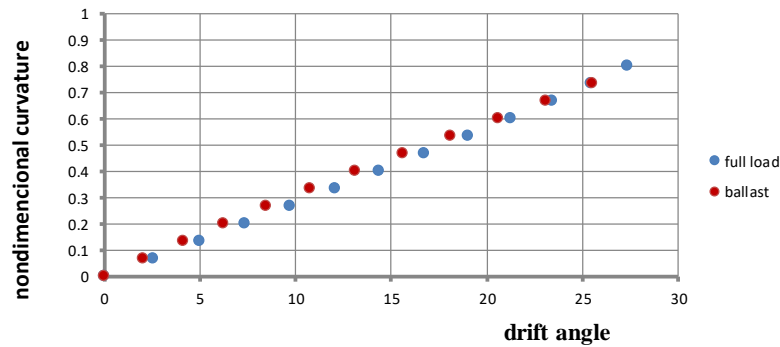


Fig.2.6. The relative curvature of trajectory at different drift angles for two trim options.

It follows from the graphs that the fully-loaded ship adopted for the study does not have the straight-line stability. However the degree of instability is small. The critical rudder angle does not exceed 2 degrees, and the diameter of spontaneous turning motions with not shifted rudder is 9 body lengths.

The relative diameter of steady turning circle with a maximum rudder angle of  $35^\circ$  is 2.6 hull lengths.

When in ballast and trimmed by the stern the ship has the straight-line stability. The minimum diameter of turning circle with a maximum rudder angle equal to  $35^\circ$  is 3.2 hull lengths.

The magnitude of the drift angle can reach  $23^\circ$ – $25^\circ$ , which is typical for ships that do not have the straight-line stability.

***Calculation of parameters of the ship entry into turning circle.*** For the values of the hydrodynamic characteristics that were used when calculating the controllability diagram, trajectories of motion and drift angles were calculated when the ship entering into a turning circle.

It was assumed in the calculations that the level-keel draft of full-loaded ship is of 4.45 m, and the ballasted ship has a trim on the stern, and the draft on the midship is 2.25 m.

When compiling a mathematical model, it was taken into account that when changing the ship trim, both geometric and hydrodynamic characteristics are changed. The calculation results in the form of motion trajectories performed for still deep water are shown in Fig. 2.7.

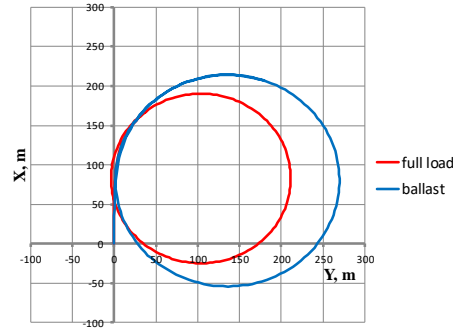


Fig. 2.7. The ship entry into turning circle in no-wind conditions

The curves show that the turning ability of the full-loaded ship is better than in ballast that is typical for displacement ships of the considered type.

The calculation results for steady and unsteady motions correspond to each other.

***Aerodynamic characteristics of ships.*** The data necessary to take into account the wind action was determined by the prototype the characteristics of which were selected from the database considering the ship hull above-water outline profile and the relative area of the above-water and underwater hull [13]. Sketches of the ship hull above-water outline profile for two trim options (fully-loaded and in ballast) are shown in Fig. 2.8.

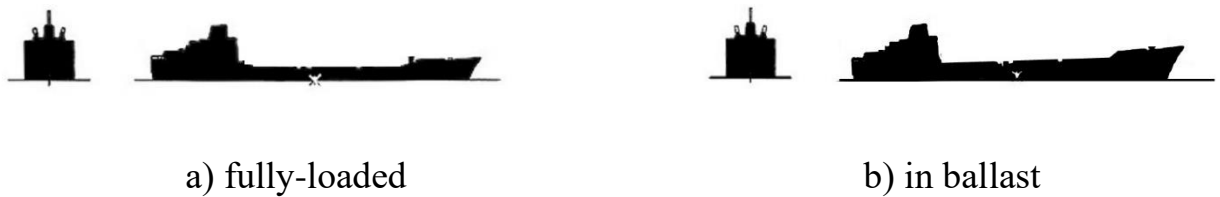


Fig. 2.8. Above-water outline profiles of the estimated ship

The aerodynamic characteristics used in the calculation are shown below in Fig. 2.9 through 2.11.

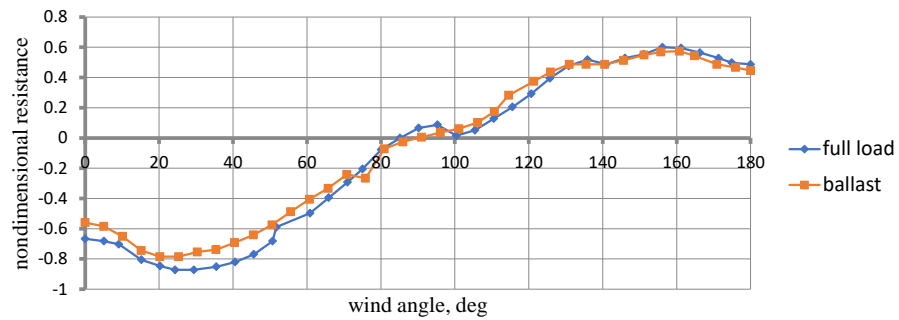


Fig. 2.9. The values of nondimensional longitudinal component of aerodynamic force at various apparent wind angles

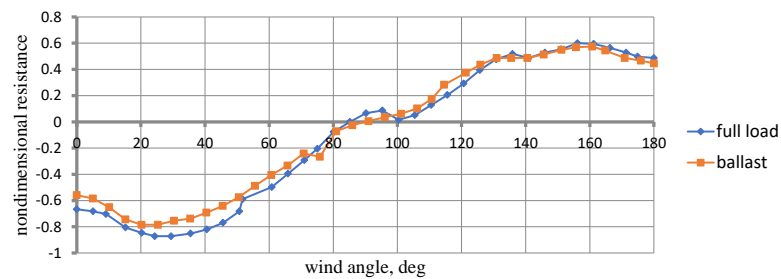


Fig. 2.10. The values of nondimensional lateral component of aerodynamic force at various apparent wind angles

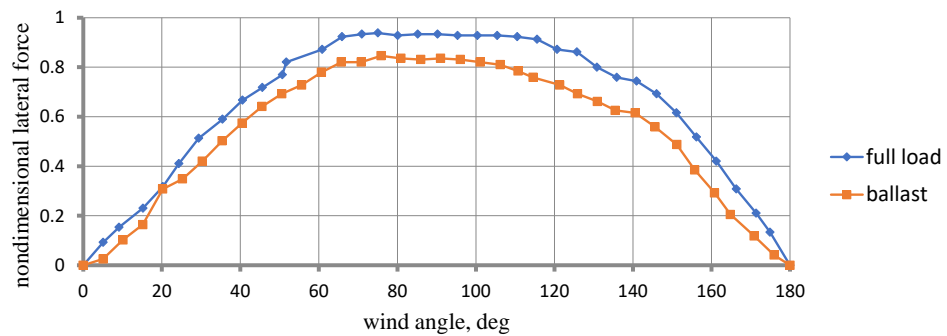


Fig. 2.11. The values of nondimensional aerodynamic moment at various apparent wind angles



## **2.2. Procedure for analyzing the possibility of a ship passage along the Saimaa Canal**

The methodology for assessing the possibility of passage along the Saimaa Canal is based on the assumption that safe operation in open water of the Canal is possible provided that the following tasks are safely performed:

1. ship passage at a specified draft and a specified guaranteed depth;
2. ship passage in all the fairway curvatures;
3. ship movement at a speed at which there is no possibility of impact with the ground;
4. ship movement at a speed limited by para. 3, in wind conditions at a maximum speed and in an arbitrary direction.

***Checking the possibility of ship passage at a specified draft and a specified guaranteed depth.*** The possibility of the ship passage along the Saimaa fairway was checked by comparing the ship draft and the guaranteed canal depth. It was thought that the under-keel clearance shall be more than 0.1 of its draft.

Provided that the guaranteed depth is 5.2 m, and the fully-loaded ship draft is 4.45 m, the under-keel clearance is 0.75 m, which is more than  $0.1 T = 0.45$ .

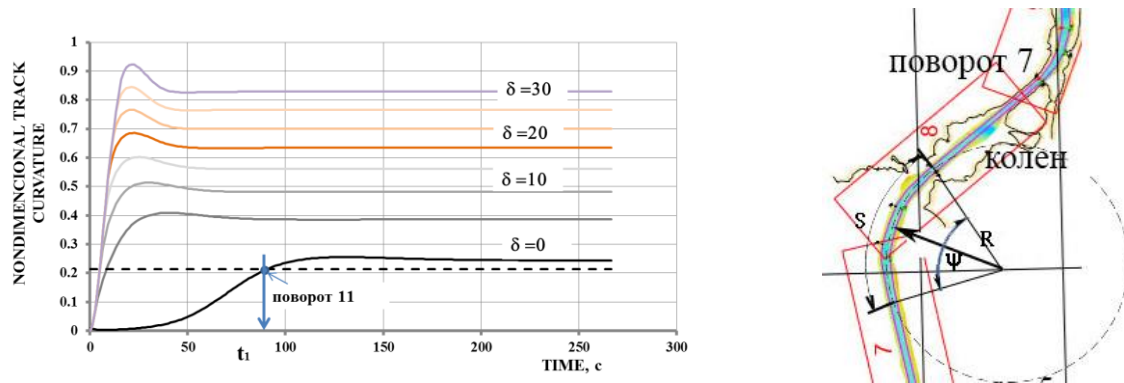
***Checking the possibility of ship passage in the canal fairway curvatures.*** The assessment of possibility of ship passage in the fairway curvatures in no-wind conditions was carried out according to the results of the calculation of maneuvers entering the turning circle at different rudder angles. The fairway relative curvature and the trajectory relative curvature that can be provided on an estimated ship steering with rudder, were compared.

The calculations were performed for fully-loaded ship. The calculation results are shown in Fig. 2.12. The calculated data are presented as changes in the relative curvature of the ship trajectory. In the same graphs the dashed lines show the relative curvature of the fairway.

The graph indicates that in no-wind conditions a fully-loaded ship can move

along the trajectory of maximum curvature with rudder angles of one to two degrees.

Therefore, in no-wind conditions, an estimated ship with a length on waterline (LWL) of 89 meters ( $L_{\max} = 92$  m) and a draft of 4.45 m can safely maneuver along the entire length of the Saimaa fairway.



a) relative curvature of the trajectory b) relative curvature of the fairway

Fig. 2.12. The change in time of the relative curvature of the trajectory. Fully-loaded ship

***Calculation of the maximum permissible speed of the ship at which there is no probability of impact with the ground.*** Assessment of the maximum permissible speed in shallow water was carried out for the fully-loaded ship for which the ratio of the reservoir depth to the ship draft is  $H/T \approx 1.2$ .

The assessment of the probability of a ship impact with the ground was carried out using curves [14], [15] of Dunde and Fergusson who have investigated this problem in detail. According to [15] the values of the ship draft at different speeds can be calculated by the formula

$$\frac{\Delta T}{L} = (0.027 - 0.152 \cdot F_{nh} + 1.894 \cdot F_{nh}^2) \cdot 0.01, \quad (2.28)$$

Where  $\frac{\Delta T}{L}$  — ship draft coefficient,  $F_{nh} = \frac{V}{\sqrt{gh}}$  — depth-Froude number.

The probability of impact with the ground is estimated as the difference between the under-keel clearance and the draft value.

***Estimated assessment of the ship safe passage in wind conditions and determination of the permissible ship speed.*** The ship motion parameters in wind conditions were determined using the equations given in paras. 2.1.1 and 2.1.2. The integration of equations was performed numerically using the Euler method.

The movement was vizualized on a microsimulator developed by the AMSUMIS. The area map was prepared using the data of the canal technical passport (Fig. 2.13) and sounding board (Fig. 2.14).

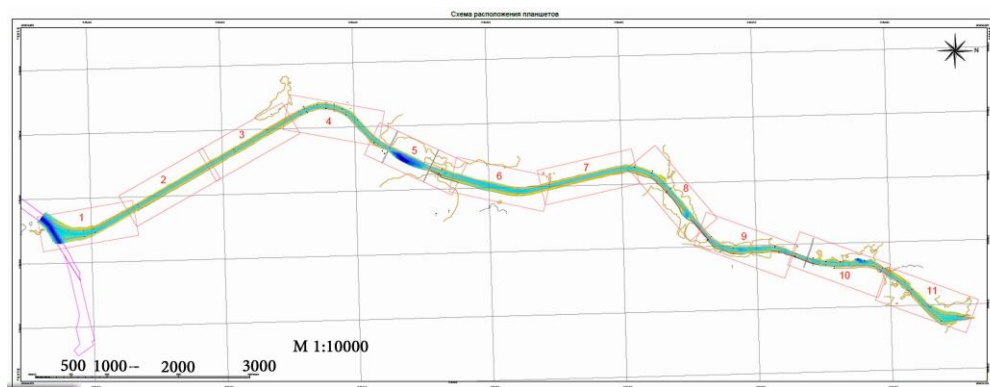


Fig. 2.13. Map of the investigated area

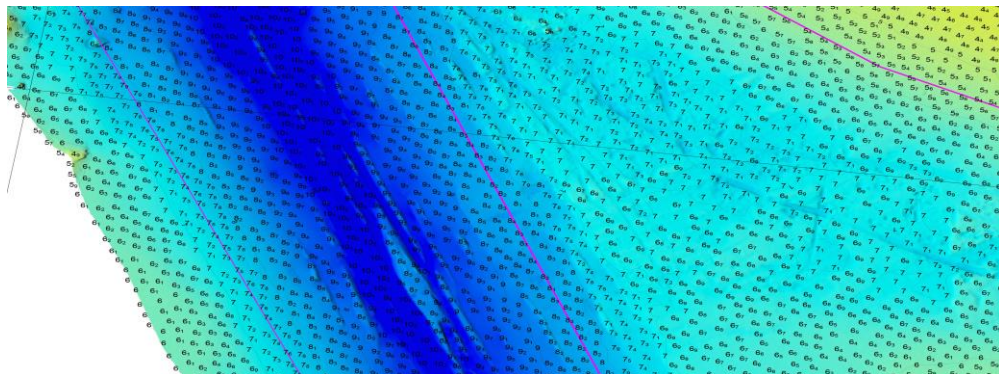


Fig. 2.14. View of one of the sounding board sheet

Data on the area in the form of a coastline (Fig. 2.15, a blue curve), fairway line (Fig. 2.15, a green curve), and constant depth lines (Fig. 2.15, a thin blue curve) corresponding to the guaranteed depth were entered to the program.

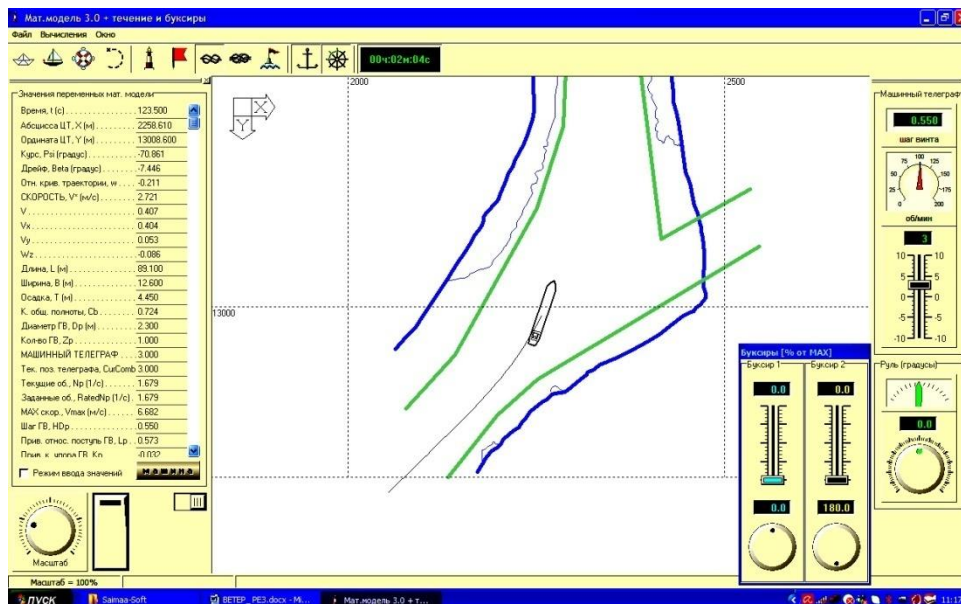


Fig. 2.15. Microsimulator screen. The test ship entry to the first turn of the Saimaa fairway. No wind conditions.

The wind speed and direction were changed in the calculations. The list of varied options for movement conditions is given in Table 2.

The ship was controlled by the rudder, with the exception of the case of movement in the north wind contributing to the ship decelerating.

The current effect was not taken into account.

*Table 2.1*  
*The list of variable parameters.*

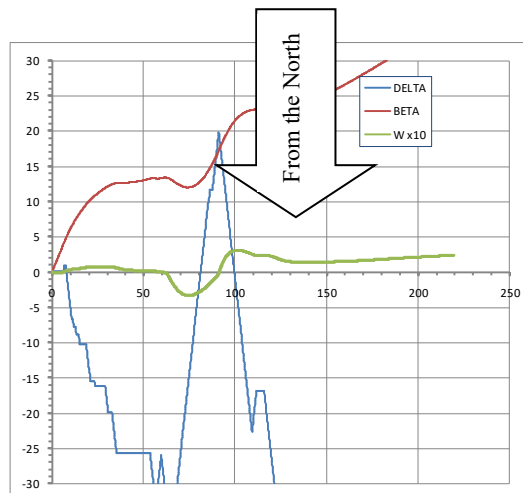
		$V_w=12$ m/s	$V_w=15$ m/s	$V_w=15$ m/s
Fully-loaded	East wind	<b>X</b>	<b>X</b>	<b>X</b>
	South wind	<b>X</b>	<b>X</b>	<b>X</b>
	West wind	<b>X</b>	<b>X</b>	<b>X</b>
	North wind	<b>X</b>	<b>X</b>	<b>X</b>
In ballast	East wind	<b>X</b>	<b>X</b>	<b>X</b>
	South wind	<b>X</b>	<b>X</b>	<b>X</b>
	West wind	<b>X</b>	<b>X</b>	<b>X</b>
	North wind	<b>X</b>	<b>X</b>	<b>X</b>

The task of the estimated ship entering only into the first turn but at all wind values was considered. It was assumed that as the deeper into the Saimaa fairway, the wind speed decreases. Therefore, extending the result to the entire area, we assess the possibility of passing along the fairway as a whole with an error in the safe direction.

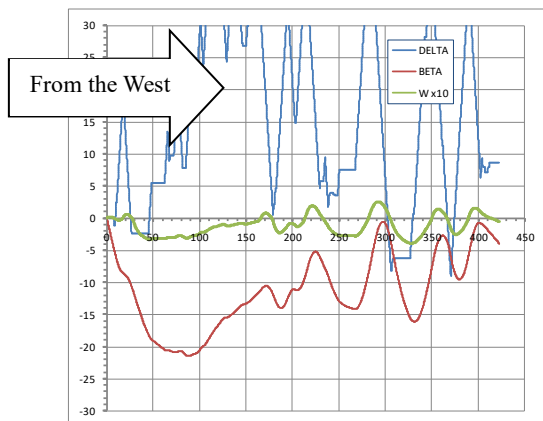
The results are presented graphically as a function of the time of the drift and rudder angles, and the relative curvature of the trajectory in Figures 2.16 through 2.18 (for fully-loaded ship). Blue curves determine the change in the rudder angle during the turn passage. Brown curves determine drift angle values. Green curves determine the relative curvature of the trajectory during the turn passage.

Averaged design values are summarized in Table 2.2.

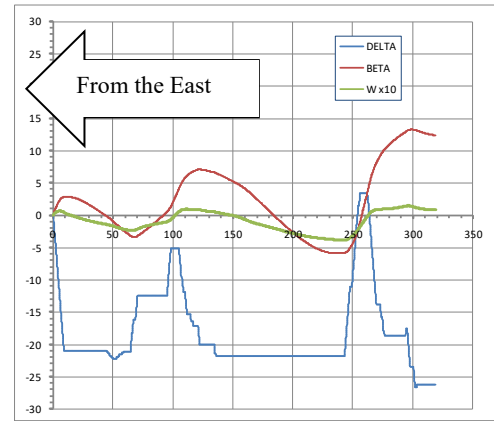
Fully-loaded. Wind of 18 m/s



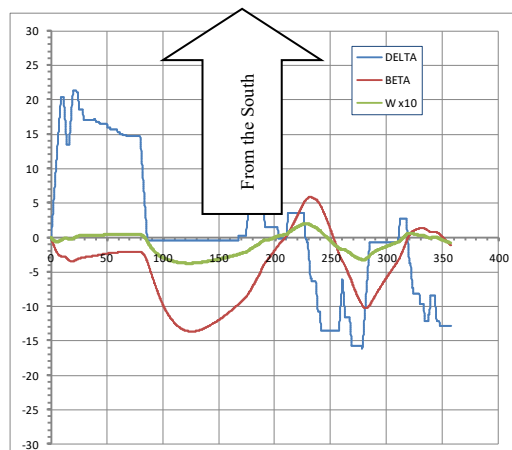
a) Wind from the North



b) Wind from the West



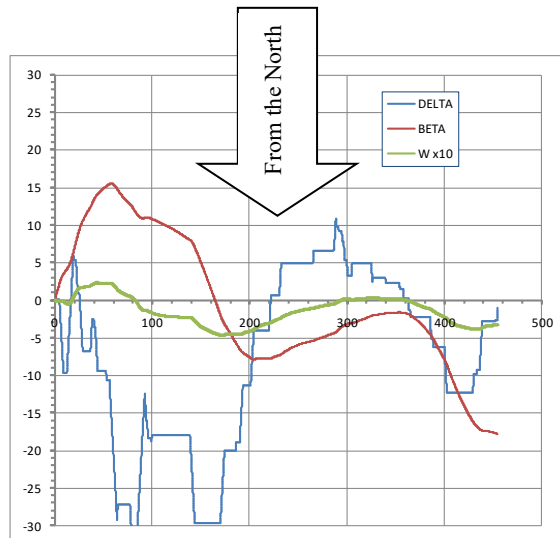
c) Wind from the East



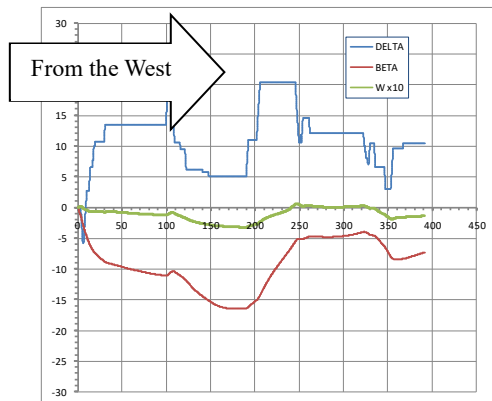
r) Wind from the South

Fig. 2.16. The fully-loaded ship motion parameters at a wind of 18 m/s.

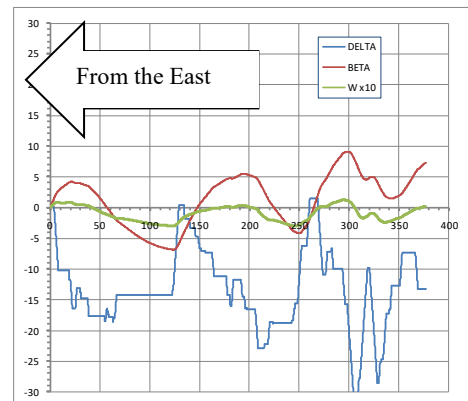
Fully-loaded. Wind of 15 m/s



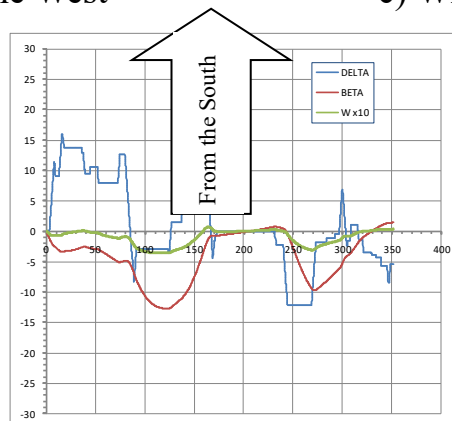
a) Wind from the North



b) Wind from the West



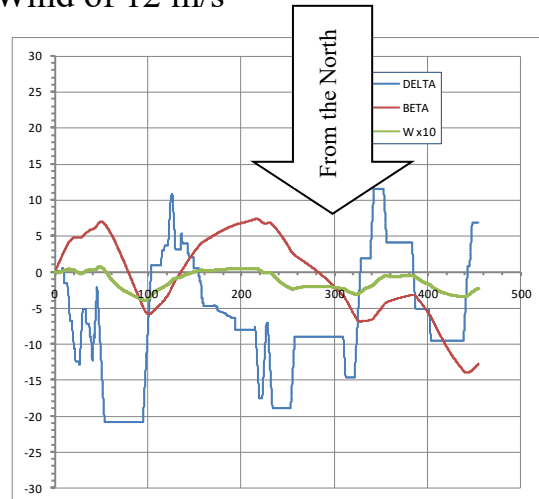
c) Wind from the East



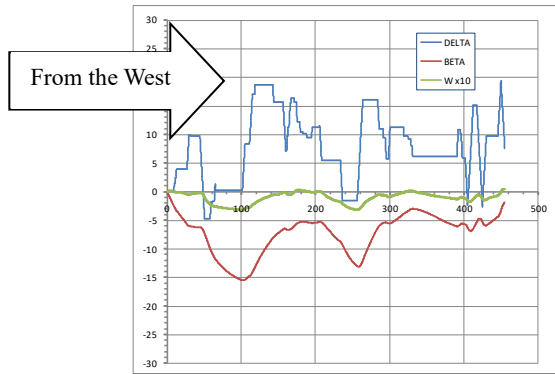
r) Wind from the South

Fig. 2.17. The fully-loaded ship motion parameters at a wind of 15 m/s.

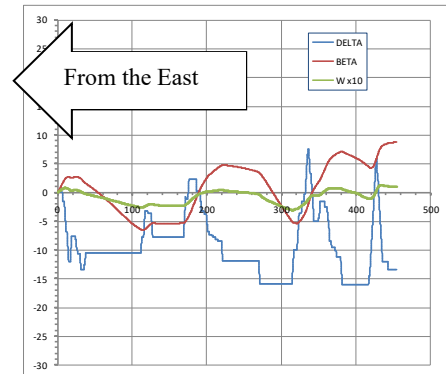
Fully-loaded. Wind of 12 m/s



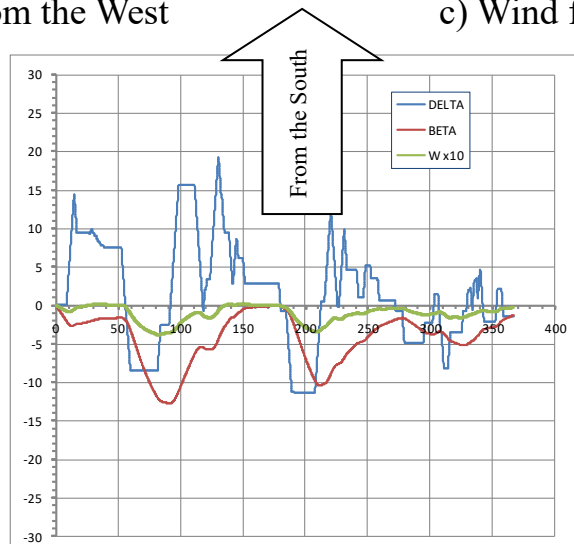
a) Wind from the North



b) Wind from the West



c) Wind from the East



r) Wind from the South

Fig. 2.18. The fully-loaded ship motion parameters at a wind of 12 m/s.



Table 2.2

*The main parameters of the ship passage of the first turn of the Saimaa fairway*

FULLY-LOADED		Mean rudder angle, deg	Mean drift angle, deg	Mean curvature of trajectory
$V_w=18$ m/s	East wind	-20	$\pm 5$	-0.3
	South wind	$15 \div -10$	$-10 \div -5$	-0.3
	West wind	30	$-20 \div 9$	-0.3
	North wind	-30	25	$0 \div +0.2$
$V_w=15$ m/s	East wind	-15	$\pm 5$	-0.3
	South wind	$\pm 9$	-7	-0.3
	West wind	14	-10	-0.3
	North wind	$-20 \div 5$	$\pm 15$	-0.3
$V_w=12$ m/s	East wind	-7.5	$\pm 5$	-0.3
	South wind	10	-7	-0.3
	West wind	10	-7.5	-0.3
	North wind	-9	$\pm 5$	-0.3

The calculations show that the winds of the Western and Northern directions at a speed of 18 m/s are the most hazardous. When a ship moves at such a wind, rudder angles reach  $30^\circ$ , and drift angle is  $20^\circ\text{--}25^\circ$ .

## **Conclusions Part 2**

A methodology was developed for assessing the possibility of a ship passing along the fairway and an assessment of its adequacy was made by calculating the parameters of the ship movement along the Saimaa Canal in the area from the Mariankivi sign to the Brusnichnoe lock. The calculation showed the efficiency of the methodology and the possibility of its distribution to the entire Saimaa Canal.

To continue work in this direction, information is needed on the areas of the Saimaa Canal that are under the jurisdiction of Finland, including a map, a sounding board sheet, and the location of the most hazardous areas for navigation. To assess the possibility of maneuvering ships in the Saimaa Canal in winter, information on the ice situation in the area of locks, as well as additional forces and moments due to ice, are required.

### 3. THE STUDY OF MAIN MOTION PARAMETERS OF SHIPS IN OPEN WATER

#### 3.1. Propulsion qualities of ships

The features of inland and mixed (river-sea) ships are determined by economic requirements and specific operating conditions [54]. The ship dimensions are strictly limited by the fairway depth, dimensions of locks and the ship channel tortuosity of the inland waterways.

At the same time, these ships are characterized by construction in large series, which contributes to a certain decrease in their construction cost. In river ship-building unification is widespread, i.e., design and construction of ships for various purposes (dry cargo ships, tankers, etc.) in the same or similar in shape hulls.

Modern inland and mixed navigation ships are characterized by full hull lines ( $0,78 \leq C_g \leq 0,87$ ), a large relative breadth ( $B/T > 3$ ) and a significant length of the parallel body (up to 60 %  $L$ ).

The draft of river ships is limited by the guaranteed navigable depth and does not exceed 3.7 meters in the conditions of the Unified Deep-Water System of Russia. For mixed river-sea ships, salt-water draft can be increased, but not more than up to 4.5 m.

The hull length of heavy ships varies between 90–145 m, which corresponds to the relationship  $6.5 \leq L/B \leq 9.0$ . Historically in Russia almost no inland navigation ships were built with a length of 85 to 95 meters.

An extended parallel body of a river ship requires special attention to the hull lines in the extremities.

The most common form of the forward end of ships is the spoon bow (Fig. 3.1) with V-shaped frames, an inclined bow line and slightly convex waterlines that meet to the CL at an acute angle. The spoon bow length is usually equal to 0.3  $L$ .

Recently on some mixed navigation ships bulbous bows have begun to be

used (Fig. 3.2), which allow to increase the ship displacement by 4–5% compared with a spoon-shaped bow with the same hull dimensions. An even larger increase in the carrying capacity of inland and mixed navigation ships with their limited dimensions can be achieved by the cylindrical shape of the bow end with significant U-shaped frames, a vertical bow line and convex branches of the waterlines that meet the CL at the right angle. For ships with such a cylindrical bow the presence of a surge wave is characteristic, which significantly increases their resistance.

The traditional aft contours of river heavy ships are sea sled lines with a small deadrise (Fig. 3.3), and for mixed navigation ships — spoon contours (such as a “small spoon”) with U-shaped frames, the bottom branches of which are sometimes straight (Fig. 3.1). The promising form of stern contours with elliptical frames and flat buttocks (see Fig. 3.2), which provides favorable conditions for the rational layout of the propulsion and steering system and increase the propulsion coefficient, is increasingly being used on heavy ships in recent years.

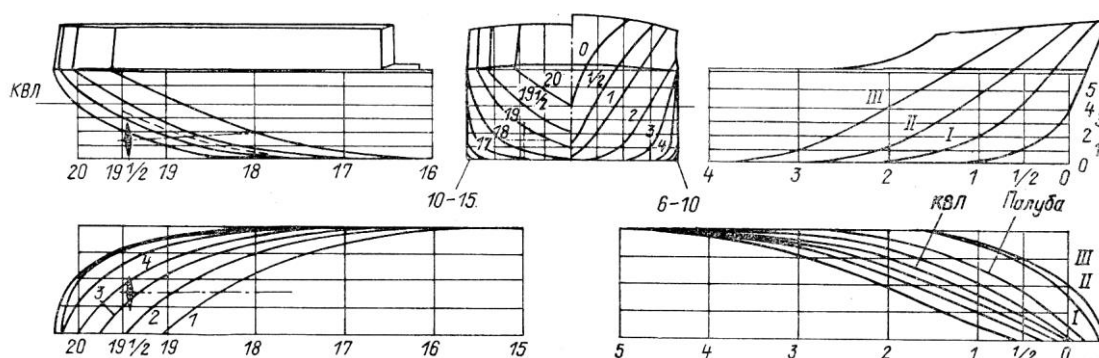


Fig. 3.1 The line drawing of a mixed navigation ship of the Volgo-Balt type. Spoon bow. Spoon stern.

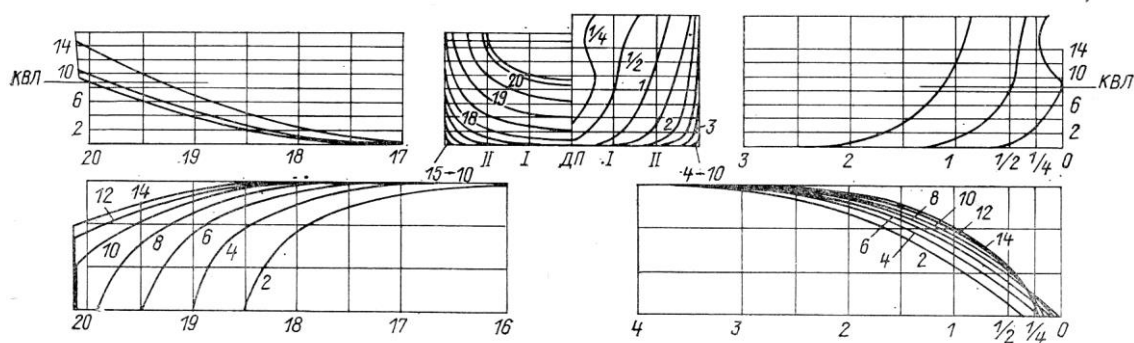


Fig. 3.2. The line drawing of a mixed navigation ship of the Manych type. Bulb bow. Elliptical stern.

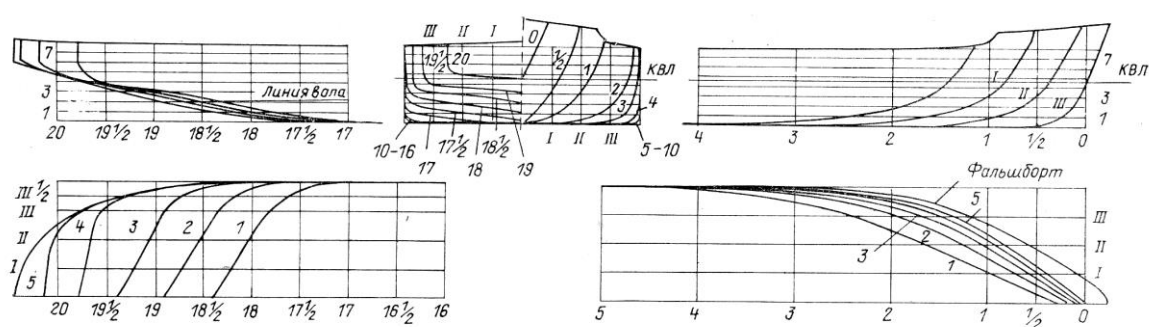


Fig. 3.3. The line drawing of a river ship of the Volgo-Don type. Spoon bow. Sea sled stern.

Heavy inland and mixed navigation ships have relatively slow speed — their operational speed in deep water is  $18 \div 22$  km/h ( $Fn = 0.16 - 0.20$ ). Despite the great fineness of these ships, their aft end when moving in deep water and in shallow water ( $H/T > 3$ ), as a rule, is subjected to a fully-wetted flow; sometimes only small local separation points can occur under the influence of operating propellers. In this case, the major part of the naked ship hull resistance ( $75 \div 85\%$ ) is of a viscous nature, while the wave component is small ( $15 \div 25\%$ ). When determining the resistance of such ships in deep water by recalculating the data of model tests according to the Froude method, the fraction of residual resistance is  $30 \div 45\%$ , and the friction resistance of the equivalent plate is  $55 \div 70\%$ .

Fig. 3.4 shows the values of the residual resistance of models of river ships

with different contours of the aft end. It follows from the graph that the residual resistance practically does not depend on the aft end lines, but decreases significantly with increasing ratio of ship length to draft.

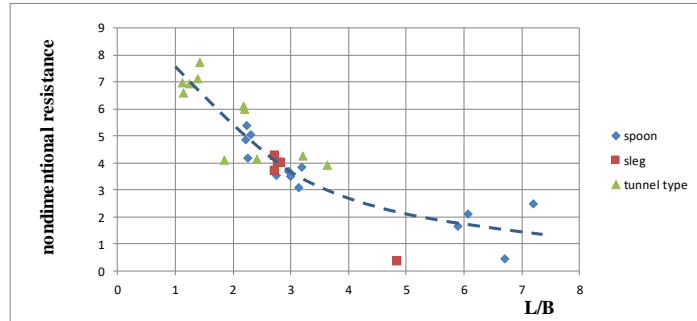


Fig. 3.4. Variation in residual resistance for river ships of various types.

In shallow water the resistance of inland and mixed navigation ships varies quite significantly depending on the relative depth.

The influence of ice conditions on the running and maneuvering qualities of inland navigation ships is practically not considered, since from the navigation completion in November until its opening in late April, the ships are at winter berthing.

### 3.2. Propulsion/steering unit

The majority of Russian river and river-sea ships are double-shaft ones, which is explained by the impossibility of delivering an optimal propeller of large diameter, on the one hand, and allows maintaining the ship controllability in case of failure of one of the engines, on the other hand.

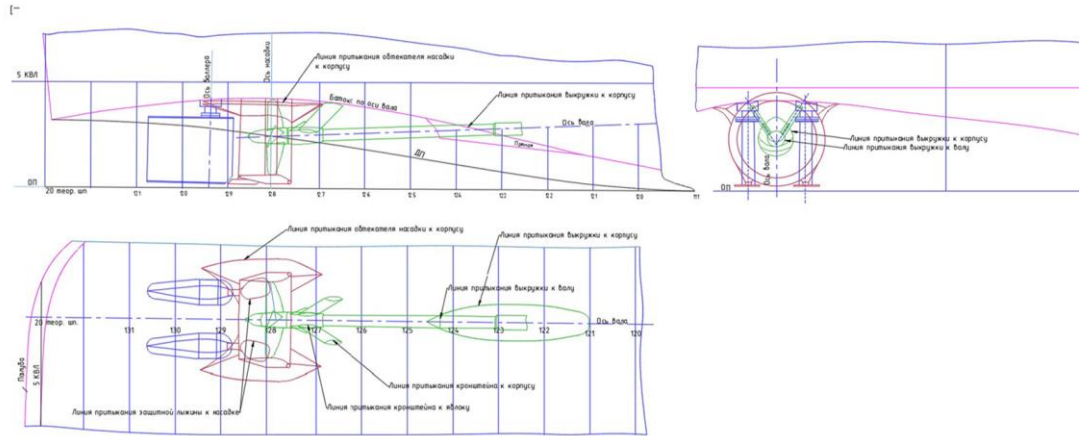
For the analysis of the propulsion and steering complex type 8 ships of various purposes and main dimensions were selected [18 ÷ 21]. The dimensions of the ships are shown in Table 1. Among the selected ships there are the following:

- Bulker for small rivers (Ship 1);
- Bulker for Enisey (Ship 2);

- Bulker – platform type (Ship 3);
- Bulker – platform type (Ship 4);
- Hopper barge (Ship 5);
- Hopper barge (Ship 6);
- Tanker (Ship 7);
- Tanker (Ship 8).

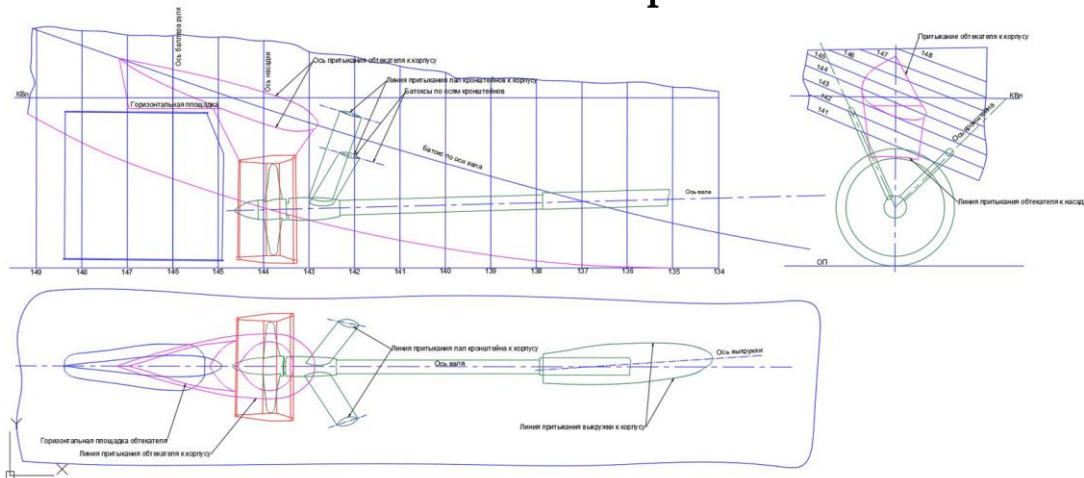
The layout of stern ends of the ships are shown in Fig. 3.5÷3.8

Ship R - 86A



Length - 78 m  
Breadth -15m  
Draft 1.4 m  
Dicplacement -1438 m<sup>3</sup>  
L/B - 5.2  
B/T - 10.7

Ship R - 97

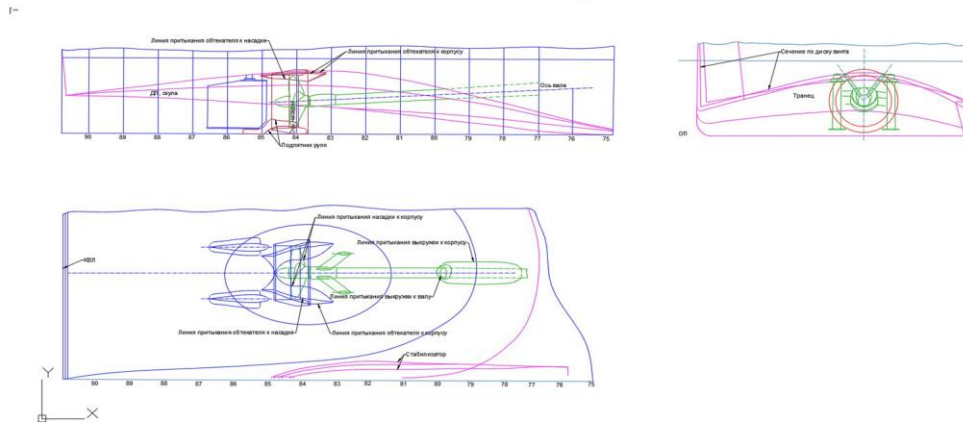


Length - 90 m  
Breadth -15m  
Draft 2.2 m  
Dicplacement -2528 m<sup>3</sup>  
L/B - 6.0  
B/T - 6.7

Fig. 3.5. River dry cargo vessels. Aft end

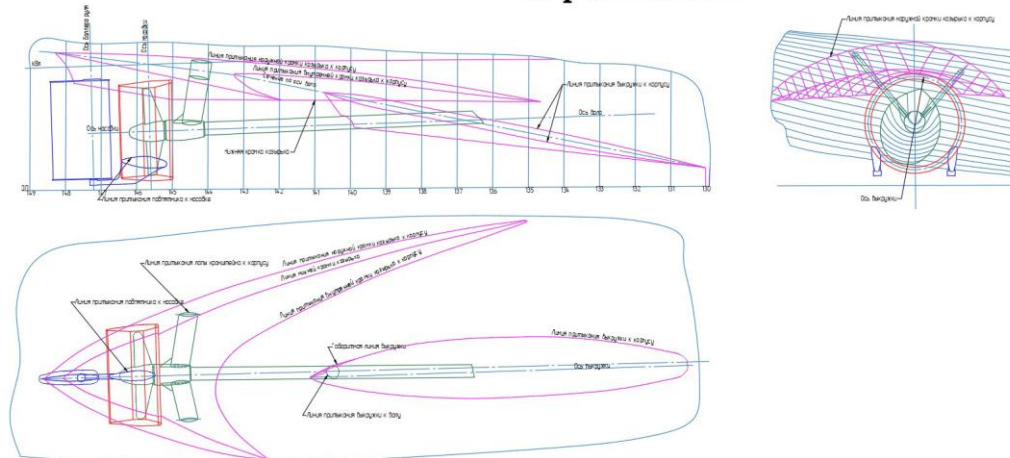


### Ship for small rivers



**Length - 50 m**  
**Breadth - 9 m**  
**Draft 1.3 m**  
**Displacement - 499 m<sup>3</sup>**  
**L/B - 5.5**  
**B/T - 6.9**

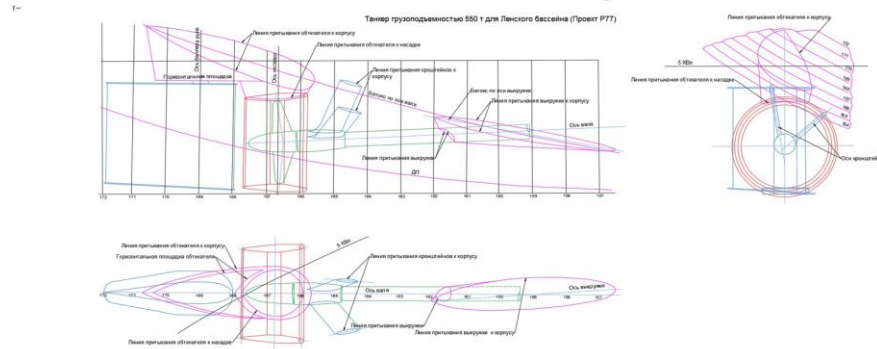
### Ship number 936



**Length - 82 m**  
**Breadth - 11 m**  
**Draft 2.2 m**  
**Displacement - 1572 m<sup>3</sup>**  
**L/B - 7.4**  
**B/T - 5.0**

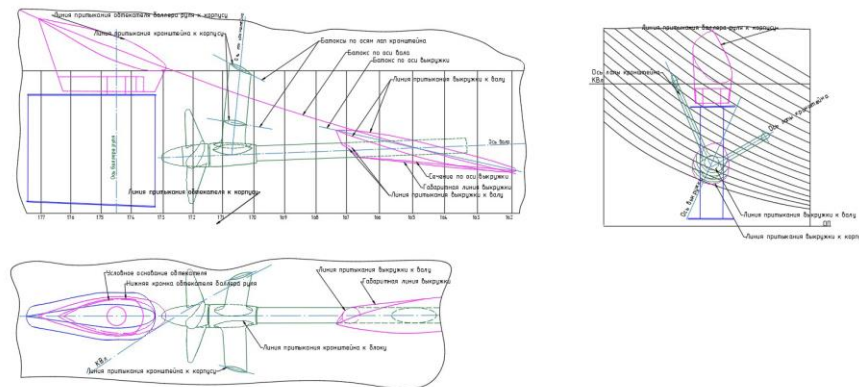
Fig. 3.6. River dry cargo platform ship Aft end

### Ship R 77



**Length - 105m**  
**Breadth - 14,8m**  
**Draft 2.5 m**  
**Dicplacement - 3210m<sup>3</sup>**  
**L/B - 7.1**  
**B/T - 5.9**

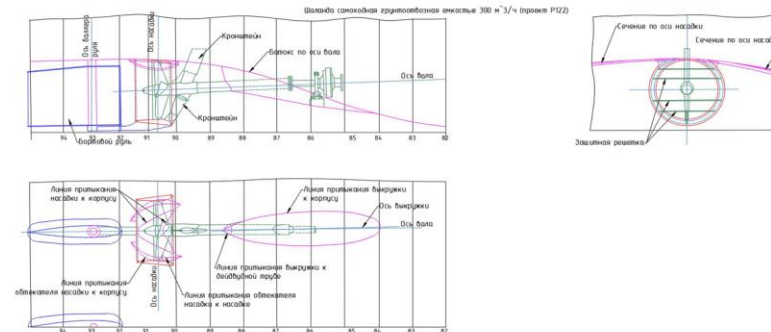
### Ship R130



**Length - 108m**  
**Breadth - 14,8m**  
**Draft 2.5 m**  
**Dicplacement - 3307m<sup>3</sup>**  
**L/B - 7.3**  
**B/T - 5.9**

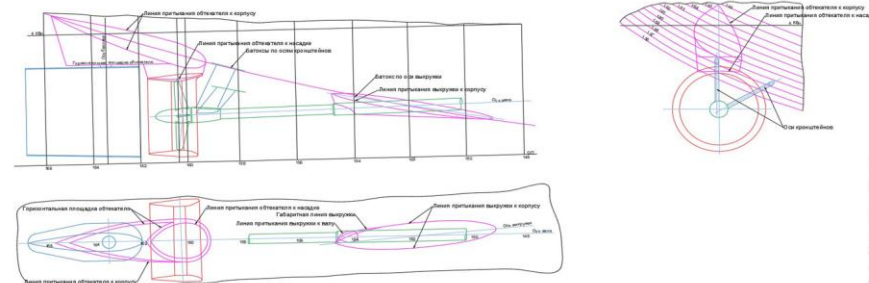
Fig. 3.7. River tanker. Aft end

### Ship R 122



**Length - 53m**  
**Breadth - 10.2m**  
**Draft 2.25m**  
**Displacement - 818.5m<sup>3</sup>**  
**L/B - 4.9**  
**B/T - 4.5**

### Ship R 32, R 32a



**Length - 96m**  
**Breadth - 14.8m**  
**Draft 3.0m**  
**Displacement - 3530 m<sup>3</sup>**  
**L/B - 6.5**  
**B/T - 4.9**

Fig. 3.8. Self-propelled hopper. Aft end

Table 3.1

*The main dimensions of the test ships.*

	Ship 1	Ship 2	Ship 3	Ship 4	Ship 5	Ship 6	Ship 7	Ship 8
	P-1437	P-936	P-86A	P-97	P-122	P-32A	P-77	P-130
Length, L	50	82	78	90	50	96.6	105	108
Breadth, B	9	11	15	15	10.2	14.8	14,8	14,8
Draft, T	1.3	2.2	1.4	2.25	2.25	3.0	2,5	2,5
Displacement	499.4	1572	1438	2528	818.5	3530	3210	3307
Coefficient, $C_b$	0.854	0.792	0.88	0.832	0.713	0.823	0.826	0.828
L/B	5.5	7.5	5.2	6.0	4.9	6.53	7.1	7.3
B/T	6.9	5.0	10.7	6.7	4.5	4.9	5.9	5.9

Table 3.2

*Features of propulsion/steering unit*

Project No.	Ship length	Type of propulsion/steering unit	Steering profile	Total rudder area, $\Sigma S$	$\Sigma S$ / LT
P-1437	50	2 nozzle propellers 4 steering rudders	NACA	3.14	20.7
P-936	82	2 nozzle propellers 2 steering rudders	NEZH / HEЖ	3.44	52.4
P-86A	78	2 nozzle propellers 4 steering rudders	NEZH / HEЖ	3.72	29.3
P-97	90	2 nozzle propellers 2 steering rudders	NEZH / HEЖ	4,23	47.9
P-122	50	2 nozzle propellers 3 steering wheels	NEZH / HEЖ	4,05	27.8
P-32A	96.6	2 nozzle propellers 2 steering rudders	NEZH / HEЖ	9.82	29.5
P-77	105	2 nozzle propellers 2 steering rudders	NEZH / HEЖ	9.0	29.2
P-130	108	2 open propellers 2 steering rudders	NEZH / HEЖ	8.98	30.1

The data analysis shows the following:

- river ships are equipped with a propulsion and steering complex, which can include two open propellers or two nozzle propellers and from two to four steering rudders;

- most rudders have a laminarized profile NEZH;
- elongation of the rudders is usually less than unity, which reduces their effectiveness; to increase efficiency, most rudders are equipped with end washers;
- the relative total rudder area of river ships is almost double the corresponding values for sea ships. This is a consequence of the increased requirements for the handling of these ships, which are forced to constantly maneuver in the confined water area.

It should be noted that according to the observations made during the navigation period 2019 (see para. 1), both single-shaft and two-shaft ships pass along the Saimaa Canal, the maneuverable qualities of which can vary in terms of the stability of rectilinear movement.

When assessing the safety of movement along the Canal, it is necessary to take into account the change in the stability of rectilinear motion in wind [9].

### ***Conclusions Part 3***

As a result of the analysis of existing types of ships, we can conclude the following:

1. Despite the fact that the shape of the stern frames for ships of various types is different, the body flow along the buttocks is characterized for any of them. Perhaps this explains the absence of a pronounced dependence of the residual resistance on the hull lines. At the same time, a significant decrease in towing resistance is noted with an increase in the hull length, characterized by the L/B ratio.
2. The length-to-breadth ratio is directly related to the lock dimensions, which is close to the optimal value for the ship hull.
3. The design of the propulsion steering complex and the relatively large total rudder area indicate problems with the handling of river ships.

#### **4. COMPARISON OF OLD TYPES OF SAIMAA MAX SHIPS AND SOME CONCEPT PROJECTS**

To analyze the data for the ships of the Russian river fleet, the Register Book [17] of the Russian River Register, officially published in the public domain, was used. Dry cargo ships up to 92 meters in length were selected from the Register Book. There were about 150 units of such ships.

To quantify the geometric parameters of these ships, dependencies displacement vs main dimensions were plotted.

Figures 4.1 through 4.3 show the values of the length, breadth and draft of ships on waterline depending on the displacement. Blue dots indicate the values of the main dimensions of Russian cargo ships registered in the Russian River Register. The green dots indicate the Russian ships that entered the Saimaa Canal during the navigation 2019. Ships from Europe entering the Saimaa Canal during the navigation 2019 are marked in red.

In Figures 4.1 through 4.3 almost unambiguous dependences of the overall dimensions on displacement are shown, with the exception of a number of ships 14÷15 meters wide, optimized to the most of the restrictions imposed by the dimensions of the locks of the Unified Deep Water System of the Russian Federation.

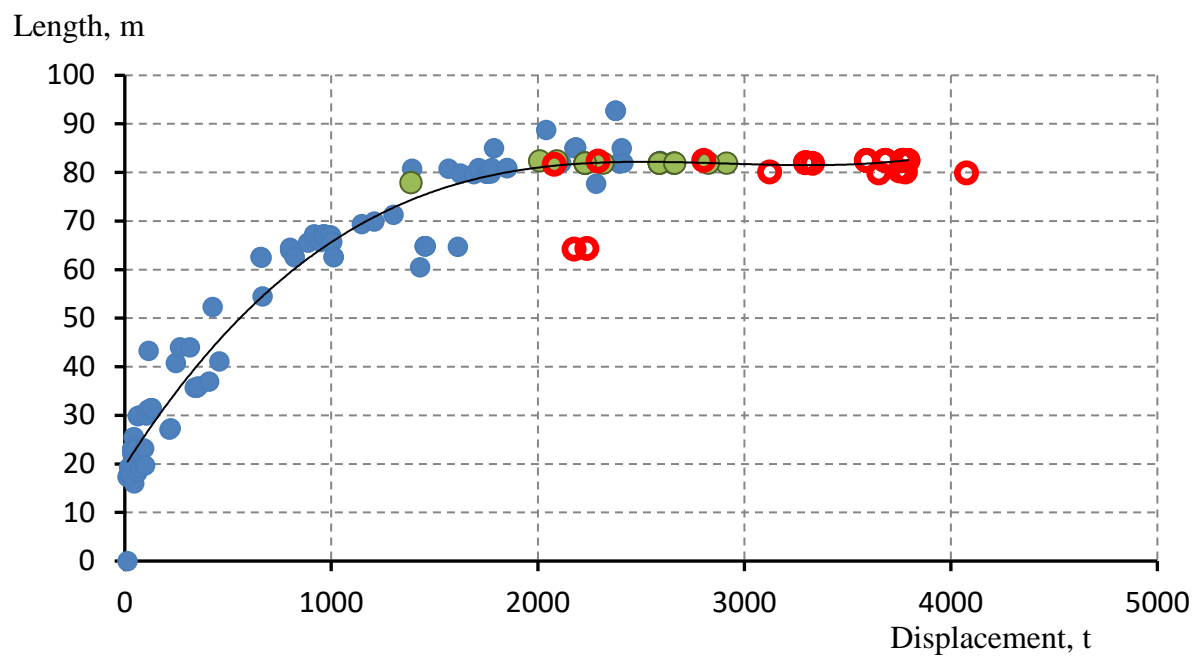


Fig. 4.1. Lengths of ships of various displacement

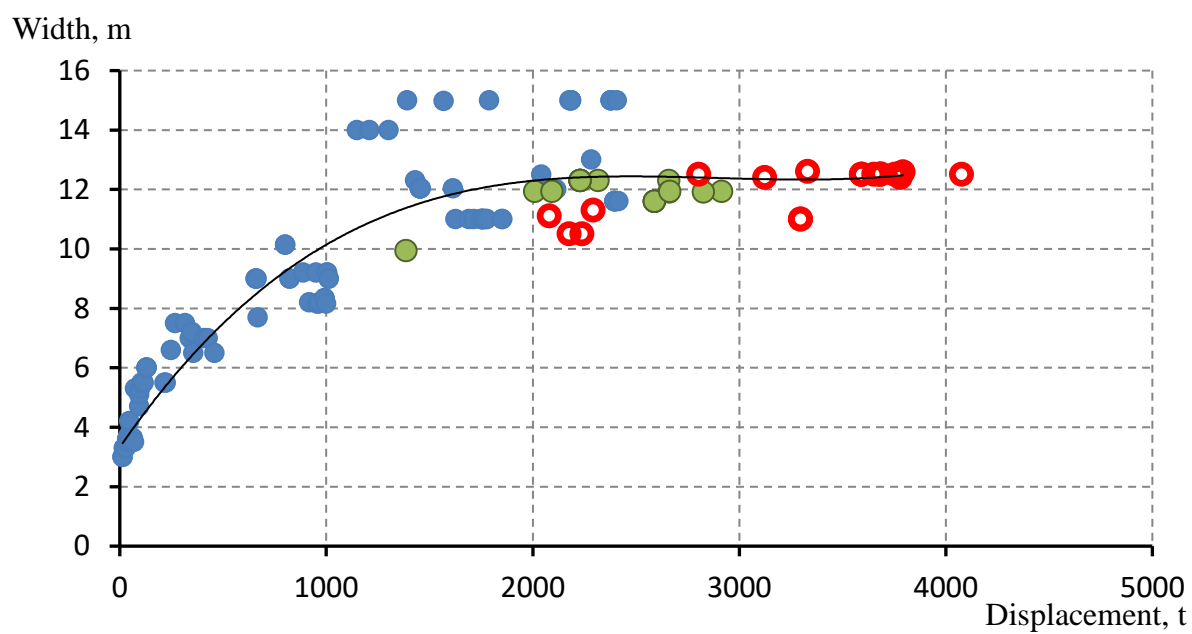


Fig. 4.2. Widths of ships of various displacement

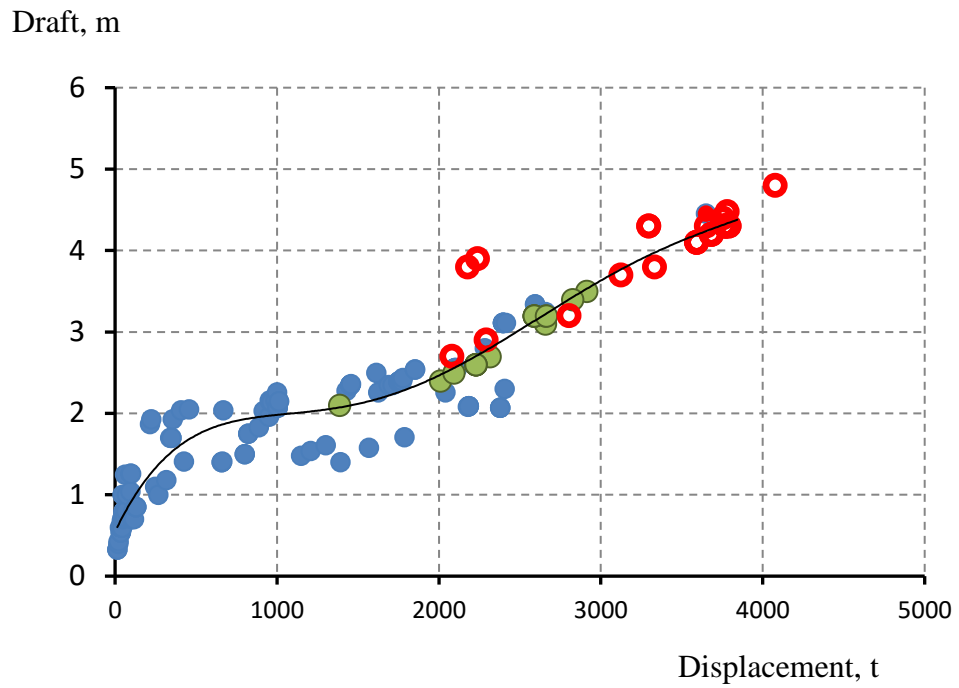


Fig. 4.3. Draft values for ships of various displacement

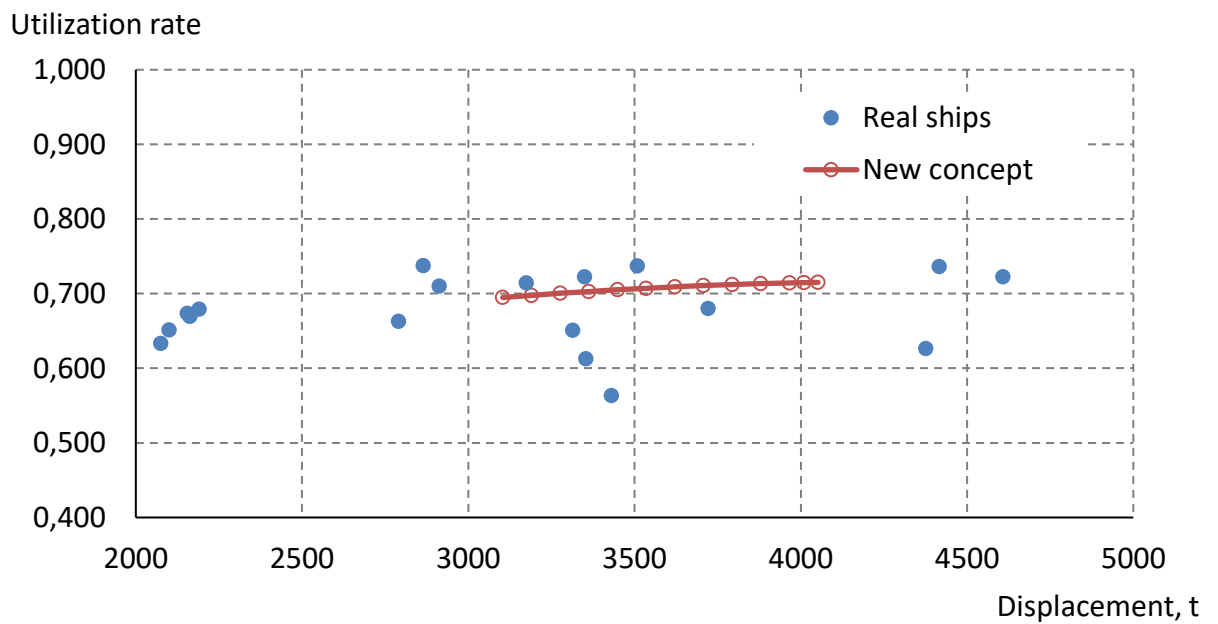


Fig. 4.5. Deadweight-displacement utilization rate

Figure 4.5 shows data on the deadweight-displacement utilization rate (Utilization rate = Deadweight / Displacement) for a number of existing ships. It also contains data related to new concept ships intended for the transport of timber cargo along lines connecting the northwestern regions of Russia with ports located



within the Saimaa water system (see Part 1 of this report). As can be seen from Fig. 4.5, new concept ships in terms of utilization rate correspond to the best models of existing ships. It can be noted that the main obstacle to a fuller use of the displacement is the route restrictions imposed by the dimensions of the locks of the Saimaa Canal and the depths of the inland waterways of the Russian Federation.

#### **Conclusions Part 4**

Based on the existing data on the composition of Russian inland and mixed navigation ships, it can be concluded that at the moment there are practically no ships corresponding to the planned dimensions of the locks on the Saimaa Canal.

Deadweight of the new concept ships will be more than 70% of the displacement; the route restrictions of the Saimaa Canal and inland waterways of Russia are the obstacles to the growth of this parameter.

## REFERENCES

1. Wentzel E. S. Probability Theory: Textbook / E.S. Wentzel. - 12th ed., stereotype — Moscow: YUSTITSIA, 2018.— 658 P.
2. Ship deployment in the directions St. Petersburg — Torovo, Torovo — St. Petersburg. Access mode: Egorov A. G. Line-by-line determination of the weight load of dry cargo mixed river–sea vessels of a new generation at the initial design stage. // Збірник наукових праць НУК, No. 3, 2013, P. 4-8
3. Standards of running time including locking and rising of bridges Torovo — St. Petersburg. Access mode: volgo-balt.ru/page/50 (reference date: 29.08.2019)
4. Russian Maritime Register of Shipping. Rules. Access Mode: <https://lk.rs-class.org/regbook/rules>
5. Russian River Register. Rules. M. 2019, 1909 p
6. Fleetphoto — Database and photographs by projects and types of ships. Access mode: <https://fleetphoto.ru/projects/61/> (reference date: 01.03.2019).
7. MarineTraffic – service for tracking ship AIS in real time. Access mode: [marinetraffic.com/en/ais/centerx:28.3/centery:60.9/zoom:7](http://marinetraffic.com/en/ais/centerx:28.3/centery:60.9/zoom:7) (reference: 29.08.2019).
8. Handbook of ship theory, vol. 3, publishing house Sudostroyeniye, Leningrad, 1985
9. A. M. Basin Ship propulsion and controllability, publishing house Transport, Moscow, 1977
10. E.P. Lebedev, R.Ya. Pershits, A.A. Rusetskiy, N.S. Avrashkov, A.B. Tarasyuk. Means of active ship control, publishing house Sudostroyeniye, Leningrad, 1969
11. Ship Theory Handbook, vol. 1, edited by Ya.I. Voikunsky, Leningrad, Sudostroyeniye, 1985
12. Manoeuvring Technical Manual, edited by Capt. Dipl.-ing. J. Brix, Hamburg, 1993.
13. A.M. Basin, I.O. Velednitsky, A.G. Lyakhovitsky. Ships hydrodynamics in shallow waters, publishing house Sudostroyeniye, Leningrad, 1976
14. Dand I.W., Ferguson A.M. The Squat of Full Ships in Shallow Water. The Royal inst. of Naval Arch., 1973.
15. Egorov G.V. Design of ships of limited navigation areas based on risk theory. — SPb.: Sudostroyeniye, 2007. – 384 P., ill.
16. The register book of the Russian River Register. Access mode: <https://www.rivreg.ru/activities/class/regbook/>

17. Reference book for serial transport ships [Text] / Ministry of the River Fleet of the RSFSR, Tech. Authority, Central Office for Scientific and Technical Information (TSBNTI) and propaganda. — M.: Transport, 1973 — 294 P.
18. Serial river vessels. Volume 8.— M., Transport, 1987 — 235 P.
19. Handbook of serial river vessels. Volume 9. M.: 1993 — 201 P.
20. Serial river vessels. Volume 11. — M., Transport, 1995 — 213 P.
21. Egorov G. V. Fundamentals of designing mixed river-sea ships // Morskoy Vestnik, No. 4 (36), 2010, 67–71 P.
22. Egorov G.V., Egorov A.G. Basic decisions for a new generation of superabundant mixed river-sea and inland cargo ships. // Sudostroyeniye, No.4, 2018, 9–15 P.
23. Egorov G.V., Egorov A.G. Forecast of the composition of the fleet of mixed river-sea ships until 2025 with the definition of the most popular types of ships // KGNTs Works, No. S2, 2018, 169–178 P.
24. Egorov G.V., Tonyuk V.I., Durnev E. Yu. Superabundant combined vessels of RST54 project for transportation of oil products and dry cargo, as well as containers, rolling equipment and project cargo. // Sudostroyeniye, No. 4 (833), 2017, 17-23 P.
25. Egorov G.V., Tonyuk V.I. Twelve multipurpose dry cargo vessels with a deadweight of 5500 tons of project 005rsd03 of the Rossiyanin type // Sudostroyenie, No. 1 (818), 2015, 9–16 P.
26. Egorov G.V. Russian shipbuilding in the XXI century // Transport of the Russian Federation, No. 4 (59), 2015, 14–19 P.
27. Decree of the Government of the Russian Federation No. 383 dated May 22, 2008 (as amended on February 25, 2014) On the Approval of the Rules for the provision of subsidies to Russian organizations for the reimbursement of part of the cost of paying interest on loans received from Russian credit organizations and a state corporation Bank for Development and Foreign Economic Affairs (Vnesheconombank) in 2009–2021, as well as for the payment of leasing payments under leasing agreements concluded in 2009–2021 with Russian leasing companies for the acquisition of civil vessels (as amended and supplemented)) // Access mode: <https://base.garant.ru/12160492/>